DEVELOPMENT OF WEARABLE TRIBOELECTRIC NANOGENERATORS USING OPTIMISED KNITTED STRUCTURES

Henarath Dassanayakalage Dumindu Geeth Dassanayaka

218131D

Degree of Master of Science

Department of Textile and Apparel Engineering

University of Moratuwa
Sri Lanka

May 2023

DEVELOPMENT OF WEARABLE TRIBOELECTRIC NANOGENERATORS USING OPTIMISED KNITTED STRUCTURES

Henarath Dassanayakalage Dumindu Geeth Dassanayaka

218131D

Thesis/ Dissertation submitted in partial fulfillment of the requirements for the degree Master of Science

Department of Textile and Apparel Engineering

University of Moratuwa

Sri Lanka

May 2023

DECLARATION

I declare that this is my own work and this thesis/dissertation does not incorporate without acknowledgement any material previously submitted for a Degree or Diploma in any other University or institute of higher learning and to the best of my knowledge and belief it does not contain any material previously published or written by another person except where the acknowledgement is made in the text.

Also, I hereby grant to University of Moratuwa the non-exclusive right to reproduce and distribute my thesis/dissertation, in whole or in part in print, electronic or other medium. I retain the right to use this content in whole or part in future works (such as articles or books).

Signature: ……..…… Date: 2023.04.18

Declaration (Supervisor)

The above candidate has carried out research for the Masters/MPhil/PhD thesis/ dissertation under my supervision.

Signature of the Supervisor: …… Date: 11.05.2023

Dr Nandula D. Wanasekara
Senior Lecturer
Department of Textile and Apparel Engineering
0University of Moratuwa.

Signature of the Co-Supervisor: …… Date: 21.04.2023

Dr Ishara G. Dharmasena,
Royal Academy of Engineering Research Fellow and Lecturer
Loughborough University
United Kingdom.

Abstract

The rapid development of portable and wearable electronic devices has increased the demand for sustainable, low-maintenance, and lightweight power-supplying methods. One of the leading technologies in fabricating such power-supplying methods is triboelectric nanogenerators, which can be used to generate electricity using human motion. Triboelectric nanogenerator works on contact electrification and electrostatic induction, and a plethora of fabrication techniques have been used in the fabrication of triboelectric nanogenerators. One such technique is knitting technology, which is one of the major textile fabrication methods.

In this research, the effect of different knitting parameters and knitted structures on electrical performance of triboelectric nanogenerators were evaluated. The knitting parameters considered are stitch length and yarn count, and knitted structures considered are single jersey, rib, and interlock. Based on the results obtained, a wearable knitted sensor was fabricated using nylon 66 and silver as triboelectric surfaces. This sensor was able to identify finger bendings and tappings. Moreover, the durability of the electrical outputs of the knitted sensor was evaluated by studying the behavior of the conductive fabric's resistance when subjected to washing and abrading. The wearable performance of the triboelectric sensor was studied by measuring the air permeability and abrasion resistance of different sections of the sensor. Finally, the capability of using the sensing fabric for IoT applications was explained.

Keywords: Triboelectric nanogenerators, Wearable energy harvesters, Knitting

ACKNOWLEDGMENT

Firstly, I would like to extend my sincere gratitude to my supervisors, Dr. Nandula D. Wanasekara and Dr. Ishara G. Dharmasena, for their encouragement and constant guidance throughout my study, which helped immensely with the success of this research.

I'm extremely grateful to Prof. W. D. G. Lanarolle for providing knowledge on knitting programming and Mr. B.T.R. Bulathsinhala for the technical support provided on knitting. Also, I would like to extend my sincere gratitude to Mr. Rameesh Bulathsinhala at Loughborough University, UK for the assistance provided in the electrical characterization of triboelectric nanogenerators. I'm grateful to Mr. S. N. Niles for granting permission to use the textile physical testing laboratory and Mrs. D.S. Dissanayake for the technical support provided in using the testing lab facilities. I wish to thank Prof. Samudrika Wijayapala for granting permission to use the wet processing laboratory and the assistance provided by Mr. C.P. Malalanayake, and Mr. K.D.T.A. Kumara in using wet processing lab facilities. I would like to thank Prof. E.A.S.K. Fernando for granting permission to obtain raw materials for the project. Also, I would like to thank Mr. J.A. Chinthaka and Mr. D. Jayasiri for the assistance provided in yarn processing. The financial assistance for this research was provided by the National Research Council of Sri Lanka, and I would like to express my sincere appreciation to them. Finally, I would like to thank my parents, the staff of the University of Moratuwa, and my colleagues for their support.

TABLE OF CONTENTS

LIST OF FIGURES

LIST OF TABLES

ABBREVIATIONS

Abbreviation	Description
IoT	Internet of things
TENG	Triboelectric nanogenerator
ATP	Adenosine triphosphate
EMG	Electromagnetic generator
PEG	Piezoelectric generators
PZT	Lead-zirconate-titanate
PVDF	Polyvinylidene fluoride
DDEF	Distance-dependent electric-field
VCSTENG	Vertical contact separation mode TENG
LSTENG	Lateral sliding mode TENG
SETENG	Single electrode mode TENG
FSTENG	Freestanding triboelectric-layer TENG
Q_{SC}	Shor circuit charge
I_{SC}	Short circuit current
V_{OC}	Open circuit voltage
SANES	Self-powered all-nanofiber-e-skin
OSAHS	Obstructive sleep apnea-hypopnea syndrome
PAN	Polyacrylonitrile
SEBS	Styrene-ethylene-butylene-styrene

SETY	Single-electrode triboelectric yarns
F-TENG	Fiber-shaped triboelectric nanogenerator
CNT	Carbon nanotube
3DB	Three-dimensional five-directional braiding
PDMS	polydimethylsiloxane
PTFE	polytetrafluoroethylene
HCOENP	Hydrophobic nanoparticles
PET	polyethylene terephthalate
FSTTN	Fully stretchable textile based TENG
PMM	Power management module
3DFIF-TENG	3D double-faced interlock fabric-based TENG
PU	polyurethane

CHAPTER 1

INTRODUCTION

The rapid advancement of contemporary technologies, namely the Internet of Things (IoT), 5G technology, wireless sensors, and wearable electronics have enabled the usage of wide range of low powered electronic devices and sensors which can revolutionize the day-to-day life of human beings by digitally connecting the world [1], [2]. With the frequent accessibility and availability to these technologies, plenty of useful applications have been realized. Among them, biomedical wearable sensors have made a remarkable impact on people's lives due to multitude of usages such as continuous health monitoring, diagnosis, disease prevention and rehabilitation [1], [2]. However, wearable sensors contain specific requirements such as being smaller in size, mobility and wearability, and lower power consumption [3]. Moreover, to deploy these sensors as a network, which can be useful for IoT applications, being able to operate in a wireless, independent, and sustainable manner is vital since there could be thousands of sensor nodes which are scattered in different areas [4], [5].

However, under the context of current technologies, sensors require a power source to carry out its functions and to transfer data to networks [4]. To this end, the essential properties of wearable sensors such as wearability, mobility and compactness are compromised by employing traditional power sources such as batteries owing to their bulkiness and rigidity. Moreover, to obtain a continuous power supply from traditional power supplies, recharging or replacing the power source is essential. But, considering the number of devices in a sensor network: which could be thousands, recharging or replacing power sources isn't viable [6], [7]. Furthermore, most of the conventional power supplies contain harmful substances such as lead, mercury, and cadmium, which makes replacing thousands of conventional power sources non–ecofriendly and unsustainable [1]. Therefore, self-powered operation of wearable sensors is crucial for the development of wearable sensor networks [1], [2], [8]. Consequently, scavenging energy from readily available ambient energy forms such as solar energy, mechanical

energy, thermal energy and converting to electricity in real-time using suitable energy harvesters is investigated as a potential method to solve aforementioned challenges.

The human body can be considered as a useful energy source for wearable applications. An average human, weighing 65 kg with 15% of body fat, has approximately 384 MJ of energy stored [9]. So, harvesting a fraction of this energy is sufficient to power up low-power electronic devices and sensors. There are a few energy types within the human body namely chemical energy, thermal energy, and mechanical energy. Especially, mechanical energy harvesting has been widely experimented for wearable sensing and energy harvesting applications [7], [10], [11].

To harvest mechanical energy, certain types of energy harvesting technologies have previously been employed namely, electromagnetic technology [12], piezoelectric technology [13], [14], and triboelectric technology [15]. Among these, electromagnetic technology is mostly used for large scale energy generation and consists of rigid components such as conductive coils and magnets, making them heavy and less wearable. On the other hand, materials and the fabrication process of piezoelectric energy harvesters is costly. Moreover, most of the high performing piezoelectric materials aren't inherently flexible [14], which is an issue when it comes to wearable energy harvesters.

Triboelectric energy harvesting technology is a relatively new mechanical energy harvesting technology, proposed in 2012 by Z. L. Wang's team [16]. This technology is formed on contact electrification, also known as, triboelectrification, and electrostatic induction. The triboelectric energy harvesters (also referred to as triboelectric nanogenerators (TENG)), in their simplest form, consist of two different dielectric material films and two conductive layers on their reverse sides which act as the two electrodes. Contacting and separating dielectric layers is the mechanism of producing an electrical signal. Compared to other mechanical energy harvesting methods, TENGs have a relatively simple structure: hence their fabrication is relatively simple, and the manufacturing cost is low. Moreover, flexible TENG structures which can scavenge energy from low frequency vibrations (<10 Hz) have been manufactured which match the frequencies of human activities such as gait cycle [17]. When

considering electrical performance, according to recent findings, higher power densities i.e., 500 Wm^{-2} have been obtained [18]–[20]. Due to these advantages, fabricating wearable TENG sensing devices is being investigated widely [14], [21]–[26][14], [27]–[32].

Despite their potential, existing TENGs lack some properties essential for wearable applications such as air permeability, stretchability, flexibility and other wearability related performances mainly due to issues with the fabrication techniques and materials. Hence, researches are conducted on improving the wearability of TENGs. One of the technologies is the fabrication of TENGs using textile materials and textile manufacturing technologies.

Textiles have been used since the beginning of civilization and the earliest evidence of textiles is dated back to seventh/sixth millennium BCE [33]. As textile materials, natural fibers (e.g. cotton, silk, jute, flax) and synthetic fibers or filaments (polyethylene, Teflon, polyester and nylon) have been used [1]. In view of fabricating triboelectric nanogenerators, aforementioned materials have the ability to be get charged upon contact electrification, hence can be used for TENG fabrication [1][17]. Considering the fabrication, textiles are mainly produced using weaving and knitting techniques, both of which have been used for TENG fabrication [1], [34], [35][29], [36]–[38]. Due to the exceptional wearable properties, textiles are becoming widely popular for wearable TENG applications.

However, at present, there is a lack of fundamental understanding on how the textile parameters and processing techniques affect the output performance of TENGs [39]. In this research, a wearable TENG device which can be used for sensing applications will be fabricated by thoroughly analyzing the relationship between textile processing parameters and the TENG output performance.

CHAPTER 2

LITERATURE REVIEW

2.1. Human body as an energy source

Similar to a machine which needs energy to power itself; the human body needs energy to function and perform day-to-day activities. The energy requirement of the body is fulfilled by the food intake. The nutrients in the food such as carbohydrate, protein and vitamins are absorbed by the digestion system and converted into glycogen (stored form of glucose), lipids and amino acids, and then diposited in the body as chemical energy [40]. When there is an energy requirement in a cell, energy storage molecules are converted into adenosine triphosphate (ATP); the energy carrying molecule which can be found in cells, to deliver energy to the destination[41]. ATP is usually consumed for three activities, which are to drive a metabolic reaction, to transport substances

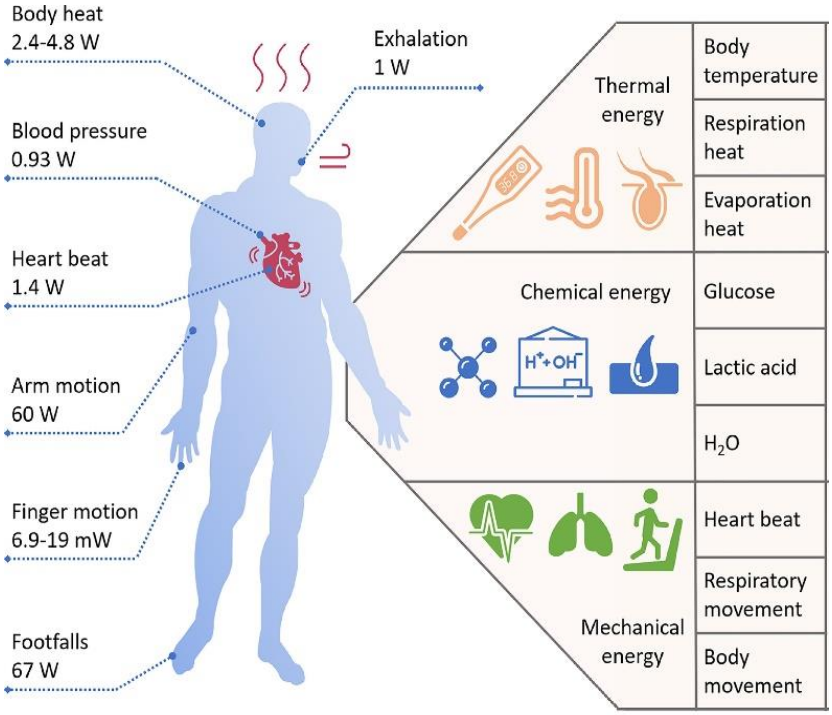

Figure 2.1: Energy generation of the human body [40]

through membranes and to perform mechanical work. Aforementioned activities again transform the chemical energy in ATP into mechanical energy for activities like walking and running, and into thermal energy to maintain body at a constant temperature. Therefore, the human body is similar to a natural energy converting factory (Figure 2.1).

2.2. Human body energy harvesting technologies.

Since the human body acts as an energy source by providing chemical energy, thermal energy and mechanical energy, the applicability of using the it for energy harvesting has been recently investigated. Several of these areas include biofuel cells for chemical energy harvesting, thermoelectric generators for thermal energy harvesting, and piezoelectric, electromagnetic and triboelectric technologies for mechanical energy harvesting. In the latter sections of the thesis, mechanical energy harvesting methods used to produce energy from the human body will be discussed in detail.

2.2.1. Mechanical energy harvesting technologies.

During daily regular activities namely walking, running, arm movements and respiration, mechanical energy is generated which can be further divided into kinetic energy, which results from rigid body movements and elastic energy e.g., breathing and heart beating: consisting of involuntary contraction and dilation movements. To harvest energy from above mentioned movements, several types of energy harvesting technologies have been implemented such as electromagnetic energy harvesting, piezoelectric energy harvesting and triboelectric energy harvesting. In the following sections of this report each of the aforementioned energy harvesting technologies are discussed with special attention to the triboelectric energy harvesting technology.

2.2.1.1. Electromagnetic energy harvesting.

The working principle of electromagnetic generator (EMG) is based on electromagnetic induction. When a conductive coil is subjected to a varying magnetic field, a current is induced in the coil creating a magnetic field against the electric field variation. According to the energy conservation principle, the electrical energy generated in the coil correlates with the work done against the force. As the main components for the energy generation of EMGs, conductive coils and permanent magnets are used, and neodymium-iron-boron magnets are typically used as permanent magnets for mechanical energy harvesting applications.

Even though EMGs are possible biomechanical energy harvesting technology, several issues remain to be fixed. As mentioned above, magnets are used to fabricate EMGs.

Owing to their rigidity, wearable properties are impaired [7]. As a solution, miniaturized magnet systems can be incorporated into EMGs. But, due to the smaller size of magnets, electrical performance is reduced. Moreover, the vibrational frequency of body movements (below 10 Hz) is lower than the resonate frequency of the EMG which is the frequency of operation to obtain the highest power output [21], so that the generated output power of the electromagnetic generator will be reduced. To minimize above issues, researchers have fabricated hybridized electromagnetic harvesters with piezoelectric and triboelectric technology [42].

2.2.1.2. Piezoelectric energy harvesting.

The piezoelectric effect can be described as the capability of certain materials to separate electrical charges when a mechanical stress is applied. This phenomenon can be seen in inorganic crystals, polymers and some biological matter such as bones [43]. The reverse effect of this can also be seen, when above mentioned type of material is exposed to an electric field which generate a mechanical strain.

Piezoelectric generators (PEG) are used to generate electricity from body movements. Lead-zirconate-titanate (PZT) and polyvinylidene fluoride (PVDF) are some of the common piezoelectric materials used to fabricate PEGs. From the above PZT has a higher energy conversion efficiency, however, PZT is rigid and heavy. So, PEGs manufactured from PZT are not ideal for wearable applications, meanwhile PVDF exhibits suitable properties for wearable applications, such as flexibility and mechanical robustness. As applications of PEG in wearable energy harvesting, a device that can harvest energy from walking (heel strike) has been fabricated by Qian and the team [44]. This device was able to deliver 9 mW (per shoe) at a walking speed of 4.8 km h^{-1}.

Even though PEGs provide better solutions for wearable energy harvesting applications compared to EMGs, there are several challenges to overcome. Similar to the EMGs, PEGs have a higher operational frequency, so, harvesting energy from low frequency activities like human motion is inefficient [17]. Moreover, harvesting energy from multi-dimensional human movements is inefficient when common linear PEGs are used. Finally, there is a lack of wearability, flexibility and biodegradability

for PEGs when employing ceramics-based high performing materials, which are also brittle and rigid. Some of these materials are lead based which is environmentally unsustainable.

2.3. Triboelectric energy harvesting.

Triboelectric nanogenerator (TENG) is a recently developed energy harvesting technology compared to EMGs and PEGs. This technology, established on tribo electrification and electrostatic induction [1], was introduced in 2012 by Wang and the team [16]. Here, a relatively simpler mechanism is employed to generate electricity. The simplest form of a TENG is comprised of two dissimilar dielectric materials, which are adhered to electrodes, separated by a thin air gap. When dielectric materials get contacted with each other, the two surfaces acquire electrostatic charges due to the transfer of electrons, ions and charged particles from one surface to another. This phenomenon is known as contact electrification or the triboelectric effect [2]. The net charge being positive or negative varies on the relative placement of the two dielectric mediums in the triboelectric series. The potential of a material to be triboelectrically charged with regard to a reference surface is utilized through empirical observation to form the triboelectric series (Figure 2.2). When a dielectric material in the top of the triboelectric series gets contacted with the one in the bottom, the prior material becomes positively charged, and the latter gets negatively charged. When an external force separates the triboelectrically charged surface, a voltage is created across the electrodes of TENGs due to the electrostatic induction generated by the separated charges on the respective electrodes. Hence, to maintain the electrostatic equilibrium, the free electrons in electrodes flow through the external circuit which connects the two electrodes, generating an output current. When considering wearable energy harvesting techniques, TENGs process certain advantages compared to energy harvesting counterparts, namely the light weight, simple structure, flexibility, and high instant power density at low frequencies [1]. Hence, TENGs are identified as a leading candidate for wearable energy harvesting and the rest of the report is focused on TENGs.

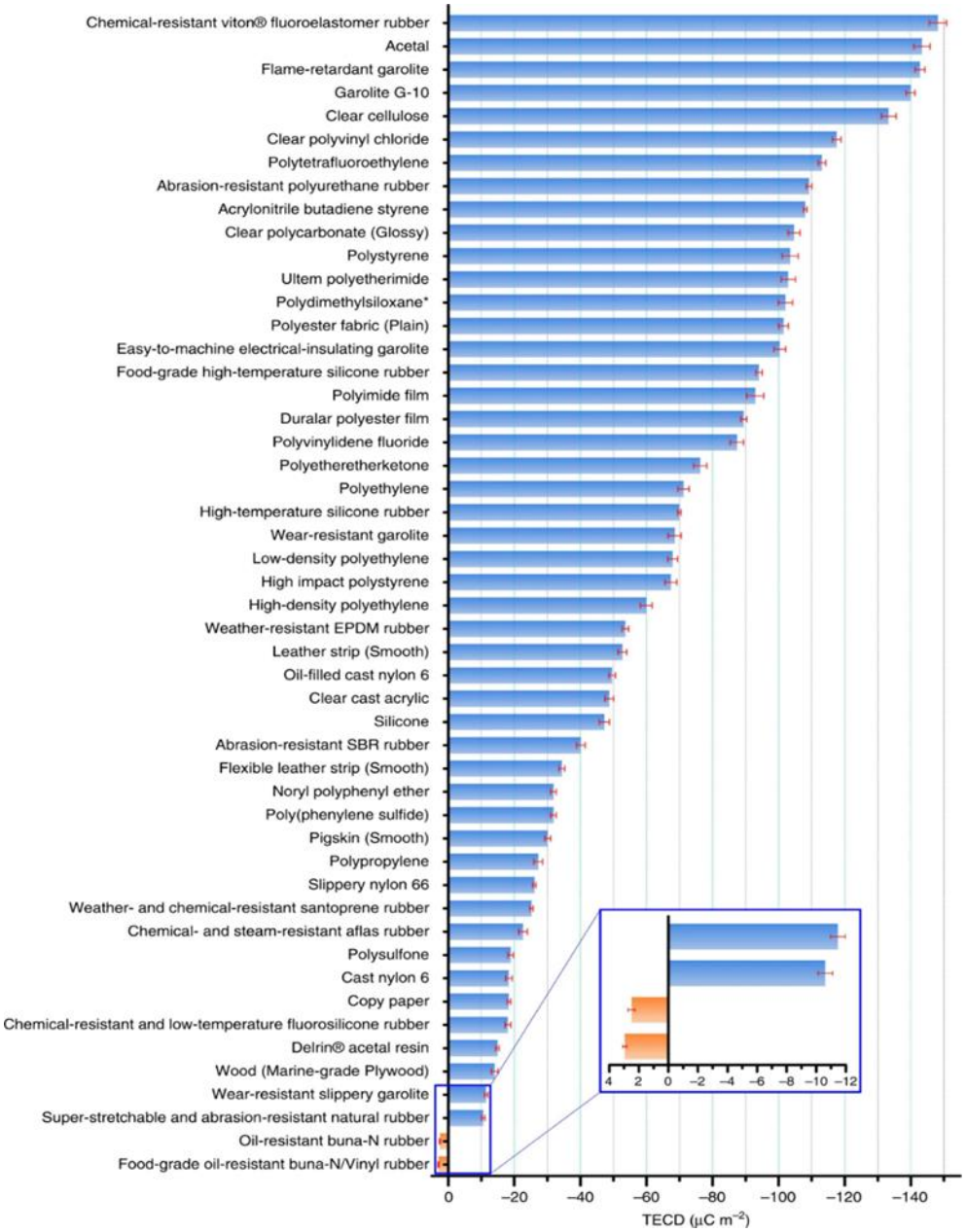

Figure 2.2: An example of a quantified triboelectric series [95]

2.3.1. Theory and working principle of triboelectric nanogenerators.

As mentioned above, a TENG usually consists of triboelectrically charged surfaces along with electrodes [45]. The charged TENG surfaces move relative to each other during the electrostatic induction phase, which creates varying electric fields at the electrode interfaces [46], [47]. This varies the electrostatic potentials on the electrodes, which generates TENG electrical outputs [8], [46]–[49]. Therefore, the TENG output generation is governed by Maxwell's displacement current:

$$J_D = \frac{\partial D}{\partial t} = \varepsilon \frac{\partial E}{\partial t} + \frac{\partial P_S}{\partial t} \quad (2.1)$$

In Equation 2.3.1, J_D represents the displacement current density, t the time, D the displacement field, E the electric field, P_S the polarization of the medium and ε the permittivity.

Modelling and simulation of the output generation of a TENG was originally done using the parallel-plate-capacitor model [50]–[53]. This model was developed linking the voltage (V), charge (Q) and layer separation (x) of the TENG (V-Q-x relationship), represented by

$$V = -\frac{1}{C(x)} Q + V_{OC}(x) \quad (2.2)$$

In Equation 2.3.2, $V_{OC}(x)$ and $C(x)$ indicate the open-circuit voltage and capacitance, respectively. This model was able to approximate the TENGs output generation behavior roughly however it was not successful in fully explaining working principles including the dielectric polarization and output induction, due to the finite dimensions of practical devices.[8], [48]

In 2017, distance-dependent electric-field (DDEF) model was derived considering the finite dimensions of the TENG surfaces and their electric field behavior, which was able to fully explain the TENGs working principles and to simulate their output generation with a relatively higher accuracy.[46]–[48], [54], [55] The DDEF model is based on the fundamental DDEF equation for a charged surface, given by

$$E_Z = \frac{\sigma}{\pi\varepsilon} arctan\left(\frac{L/W}{2(Z/W)\sqrt{4(Z/W)^2+(L/W)^2+1}}\right) = \frac{\sigma}{\pi\varepsilon} f(z) \quad (2.3)$$

In Equation 2.3.3, E_Z represents the average electric field perpendicular to the mid-point of the charged surface, L and W are the length and width of the charged surface respectively, σ is the surface charge density, ε is the dielectric constant, and z is the perpendicular distance from the charged surface at which the electric field is considered. The DDEF model considers the electric fields originating from each of the triboelectrically charged surfaces, as well as the electrode interfaces, to calculate the potential of the TENG electrodes. These potential calculations are then used to

evaluate the voltage, charge, current, and power outputs of the TENG. The electric-field-based TENG modelling and simulation has been further expanded into 3D modelling in recent years for more versatile yet complicated theoretical derivations. [56], [57]

The power generation of TENGs is affected by several key parameters. The DDEF model suggest seven primary TENG parameters directly affecting the electric fields, and thus the electricity generation of a TENG [47], [48]. These include material parameters which are the triboelectric charge density, dielectric constant, structural parameters namely, triboelectric surface area, dielectric layer thickness, and three motion parameters: frequency, amplitude, and the nature of contact during TENG layer movement [47]. The power generated by a TENG is quadratically proportional to the triboelectric charge density. Stronger electric fields are generated by higher charge densities, which induce higher outputs. Theoretically, lower the dielectric constant, there should be a higher output induction due to the better propagation of electric fields [47]. however, the opposite trend has shown in some studies [58]. Larger effective triboelectric surface areas produce higher output induction. Lower thickness is preferred for higher induced outputs hence, the reduction of the electric field is minimum while reaching the electrodes, which in turn gives higher output induction. Despite that, some studies have suggested that there is a limit for minimizing the thickness of the dielectric layer since electrostatic charges should remain in the dielectric layer without reaching the electrode [59]. Higher the motion frequency, the output current and the produced power will increase attributed to the rapid flow of charges between electrodes. Also, higher amplitude of contact separation movement increases the output power since higher amplitudes create higher potential difference between electrodes. Maintaining an adequate/conformal contact and separation between the dielectric layers increases TENG outputs since contact electrification and electrostatic induction occur sufficiently. Apart from seven primary parameters, contact force/pressure of TENG surfaces, [60] humidity, [61] temperature, [62] and roughness of the triboelectric contact surfaces[63] have been identified as some of the possible secondary factors identified which can influence the electrical performance of triboelectric nanogenerators.

2.3.2. Four main working modes of triboelectric nanogenerators

According to the motion profile and structure, four working modes of TENGs have been specified: vertical contact separation mode, lateral siding mode, single electrode mode and free-standing triboelectric layer mode (Figure 2.3).

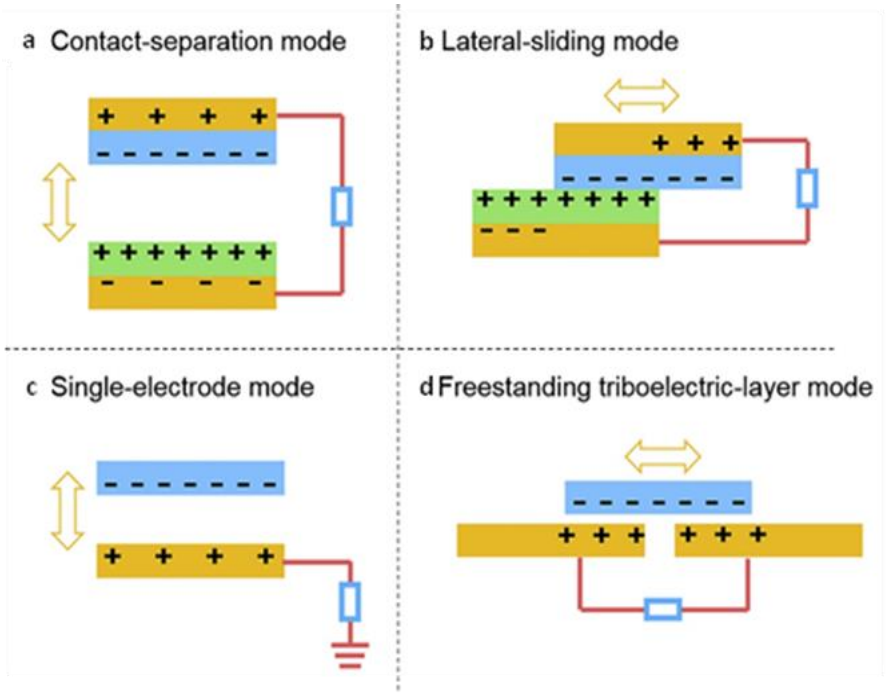

Figure 2.3: Four main working modes of TENGs, depicting (a) vertical contact-separation mode, (b) lateral-sliding mode, (c) single-electrode mode, and (d) freestanding triboelectric-layer mode. [96]

2.3.2.1. Vertical contact separation mode

Vertical contact separation mode TENGs (VCSTENG) can be divided into two subcategories: one which uses two dielectric layers as the friction surface (figure2. 3(a)) and the other uses a one dielectric layer and an electrode which act as the friction surface as well. In this mode, when two friction surfaces contact each other by the aid of an external mechanical force, charge separation occurs due to the triboelectric effect and when the friction surfaces are separated, a potential difference is induced on the electrodes. Since two electrodes are connected with each other using a conductor, charges flow from the top electrode to the bottom electrode. When the friction surfaces are further separated, the increment of the potential induced by separated charges

reaches its maximum value. So, the electron flow stops. When the distance between friction surfaces is reduced again using an external force, electrons move from bottom to top electrodes to balance out the reduction in induced potential difference between electrodes. As the two friction surfaces touch each other, the net potential difference between electrodes becomes zero and charge flow stops again. VCSTENGs can be used to harvest power from intermittent motions such as gait cycle.

2.3.2.2. Lateral sliding mode

Lateral sliding mode TENGs (LSTENG) also divide into two subcategories which are dielectric/dielectric (figure 2.3(b)) and dielectric/electrode. In the former, two friction surfaces are dielectric materials, and the latter has replaced on one dielectric layer with an electrode, hence the electrode is employed as a friction surface as well. Even though the construction of LSTENG is related to the VCSTENG, the motion of friction surfaces are different. Here, charge generation occurs as contacted friction surfaces are relatively sliding compared to each other. Let's consider the situation where both the friction surfaces are fully overlapped with each other. Since there is no net voltage difference across the electrodes, the current doesn't flow. As one friction surface has a relative movement due to an external force, overlapped area is reduced and a net voltage difference across the electrodes is formed due to the charges generated by the triboelectric effect. Hence, electrons move from the top to the bottom electrode, generating a current. When two friction surfaces are fully separated from each other, the induced net voltage difference gains its maximum value and current flow terminates, and the voltage doesn't increase further. When a mechanical force is applied on friction surfaces in the reverse direction, the induced voltage difference reduces, consequently, electrons will flow from bottom to top creating a current in the opposite direction. As the two friction surfaces fully overlap, current flow is again terminated since there is no voltage difference relating the two electrodes.

This mode of operation can be used to harvest energy from wind and water by converting them to planar movements such as disk rotation and cylinder rotation [64]. One of the most highlighted disadvantages of this mode is high friction forces applied on dielectric surfaces which reduces the durability of the device and the energy

conversion efficiency [64]. On the contrary some researchers have suggested that this mode has enhanced power output than the VCSTENG mode since the sliding movement produces more charges compared to contact separation mode [18].

2.3.2.3. Single electrode mode

Compared to VCSTENG and LSTENG modes single electrode mode TENGs (SETENG) employs one electrode for its functionality. This mode can be divided considering the movement of friction surfaces: sliding SETENGs and contact separation SETENGs. Each of the above can be further divided based on the material used for the friction surface: dielectric/ dielectric and electrode/ dielectric (figure 2.3(c)). The former uses a dielectric mounted on an electrode as one friction surface and the remaining dielectric moves freely. The latter uses an electrode which also functions as a friction surface and the dielectric material behaves the same as the previous. The working mechanism of all the above variations is same as the VCSTENG and LSTENGs except, in the single electrode mode, the electrode is grounded. When a contact separation movement or a sliding movement takes place between friction surfaces, a net difference in potential occurs between the ground and the electrode. Hence electrons move from the electrode to the ground and vice versa.

In contrast to VCSTENGs and LSTENGs, only one electrode is needed for SETENG to connect to an external circuit, which increases its versatility. On the other hand, due to electrostatic shielding of the electrode, the maximum transferred charge efficiency can only reach 50% compared with a corresponding VCSTENG or a LSTENG, which reduces SETENGs output performance [18].

2.3.2.4. Free standing triboelectric layer mode.

Freestanding triboelectric-layer TENGs (FSTENGs) were created more recently [15], [18], [45], [52], [65] and are divided into two configurations, contact-mode FSTENG and sliding-mode FSTENG (figure 2.3(d)), each of which have either a dielectric or metal freestanding triboelectric layer [15]. Freestanding TENGs' advantages include higher energy conversion efficiency, long-term stability, and minimized surface wear [18]. As a whole, contact-mode FSTENGs are able to generate electrical energy from

any external mechanical stimulus, increasing the device versatility and applicability [25].

One advantage of the sliding-mode FSTENG over the LSTENG is that it does not require direct physical contact between triboelectric surfaces, decreasing heat generation and material wear during the frictional process. Nevertheless, sliding-mode FSTENGs require the triboelectric material to be pre-charged for their correct operation. This mode features other advantages including improved energy conversion efficiency and robustness [18].

2.4. Textile based wearable triboelectric nanogenerators.

Wearable triboelectric nanogenerators require combined effect of electrical properties and wearable properties such as breathability, flexibility, washability, stretchability. Only a limited number of materials can provide both electrical properties and required properties for wearable TENGs. Since the introduction of triboelectric energy harvesting technology, numerous research has been carried out to fabricate TENGs with balanced wearable and electrical properties. Recently, textile material based TENGs have emerged as a possible candidate for manufacturing wearable TENG devices for IoT applications [1], [2] . When considering common materials used to produce textiles such as nylon, polytetrafluoroethylene (PTFE), cotton, polyethylene, and polyester, most of them possess the ability to be triboelectrically charged, which makes textile materials favorable in fabricating TENGs [1]. Moreover, different stages of textile manufacturing process such as spinning, weaving, knitting provide a variety of options to integrate triboelectric properties into textiles [1][17].

In the following sections, most recent textile based TENG developments are analyzed, which are arranged according to textile fabrication process where the triboelectric functionalization has been done.

2.4.1. Yarn/fiber based TENGs.

In this segment, textile based TENGs, which are triboelectrically functionalized in the fiber or yarn manufacturing stage are discussed. For simplicity of understanding, this section is further divided into sandwiched fiber-structures and core-shell structures.

Herein, triboelectric functionalization of textile fibers occurs in the beginning of the manufacturing process namely, in the spinning process; thus, this approach offers the advantages of the maximum control and modification capabilities for energy generation. [1] Conversely, due to the small size of fibers ranging from micro to nanometers and weak mechanical properties, handling and processing them is difficult.

2.4.1.1. Sandwiched fiber/yarn based TENG developments.

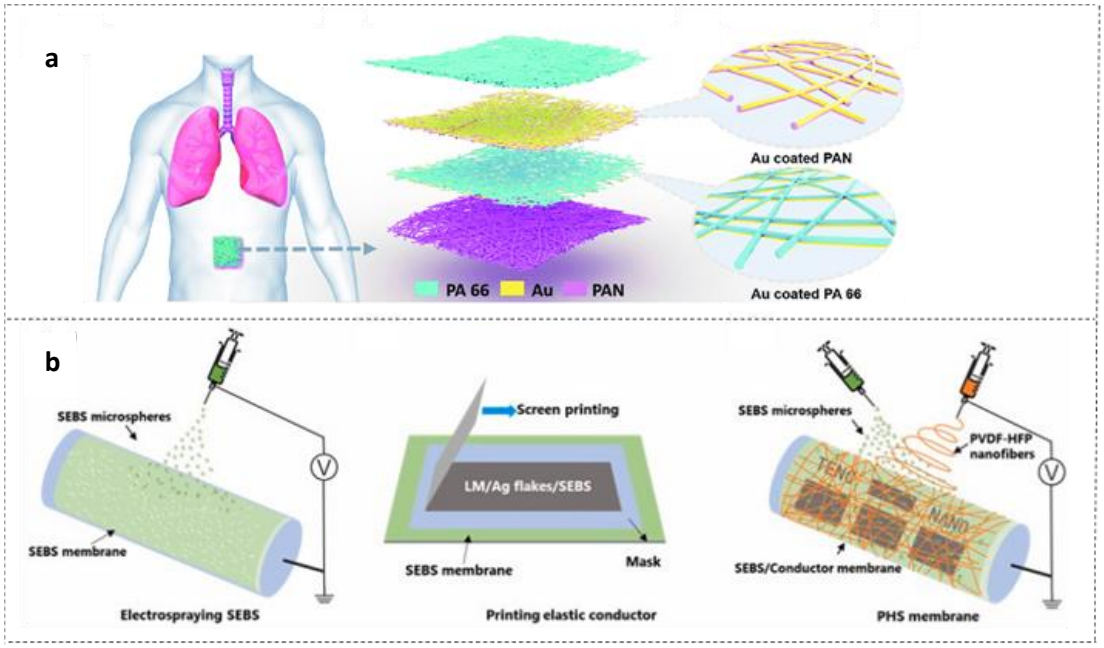

Figure 2.4: Sandwiched fiber/yarn based TENG developments. (a) An application of SANES and an enlarged view of its layers [66]. (b) The manufacturing process of mechanically interlocked nanofiber membrane based wearable TENG[67].

In this arrangement, TENGs are manufactured by placing functionalized fibers/yarns in between multiple material layers. This method is convenient for utilizing fibers and yarns which cannot be used in traditional spinning processes due to their lower mechanical properties. To fabricate these types of structures, techniques such as electrospinning are widely used. In one example, electrospinning was used to manufacture a breathable and highly sensitive self-powered all-nanofiber-e-skin (SANES) TENG (Figure 2.4(a)) for respiratory monitoring and obstructive sleep apnea-hypopnea syndrome (OSAHS) identification [66]. Here, as the positive triboelectric material, electrospun Nylon 66 fibers coated with a gold (Au) electrode were used, and polyacrylonitrile (PAN) nanofibers coated with Au were used as the

negative triboelectric material. Under a 3 Hz motion frequency and an applied load of 10 N, this device was capable of delivering an open circuit voltage (V_{OC}) of 420 V, short circuit charge (Q_{SC}) of 160 nC, and a peak power density output of 330 mW m^{-2} through a resistance of 100 MΩ. Furthermore, the nanofibers used here were tested for long-term wearing feasibility, which indicated no negative effect on human skin. The TENG was employed in respiratory monitoring by placing the device above the navel with the support of a medical bandage. It was able to identify different breathing patterns with high accuracy and reliability, and its use as a sensor to identify obstructive apnea in real-time was demonstrated.

A combination of electrospinning and electro-spraying has been utilized to produce a mechanically interlocked nanofiber membrane-based wearable TENG (Figure 2.4(b)).[67] The fabrication of this TENG was done in three steps. First, styrene-ethylene-butylene-styrene (SEBS) was electro-sprayed, and subsequently a suspension of liquid metal gallium indium tin (GaInSn) and silver (Ag) flakes in SEBS resin were screen-printed onto the previously formed SEBS membrane, which made a stretchable electrode for the TENG. To make the negative triboelectric surface, poly (vinylidene fluoride-co-hexafluoropropylene) (PVDF-HFP) was electro-spun on the flexible electrode simultaneously with electro-spraying of SEBS. The latter acted as a binder to mechanically interlock PVDF-HPF nanofibers. Also, forming SEBS microspheres layer on the electrode made it stretchable and breathable, which are important in determining the wearability of TENGs. The electrical output of the TENG was evaluated while it was operating in single-electrode mode. The 2 x 2 cm^2 TENG was able to produce V_{OC} of 85 V, short circuit current (I_{SC}) of 4 μA and Q_{SC} of 15 nC under a tapping force of 30 N at 5 Hz, and maximum power density of 219.66 mW m^{-2} through an external resistance of 20 MΩ. A significant increase of electrical outputs was observed upon stretching the TENG from 0% to 100%, which was attributed to the increment in contact area following the strain. This TENG (4.5 x 4.5 cm^2) was used to light up 200 LEDs from hand tapping motion and a 33 μF capacitor was charged up to 1.43 V within 144 seconds. Using the advantage of being waterproof, this TENG was used to harvest energy from flowing water. Furthermore, the TENG was utilized

as a self-powered e-skin for real-time human motion sensing and as a tactile interactive interface in harsh conditions.

Overall, it is evident that sandwiched fiber/yarn-based structures rely on nanofiber forming techniques such as electrospinning to obtain higher outputs due to inherent properties of nanofiber webs such as stretchability, increased surface area, and stretch-induced change of surface area. One of the specialties of fiber sandwiching method is, it allows to use fibers with poor mechanical properties, yet having high triboelectric properties for TENG fabrication.

Even though using fiber sandwiching for TENG fabrication offers excellent triboelectric properties and mechanical properties, the are some drawbacks in this method. As mentioned above, in this configuration, nanofibers have been used as triboelectric materials and producing nanofibers is still done in lab scale. Also, significant time is needed to fabricate high quality nanofiber membranes with adequate thickness which diminishes the scalability of this method. In addition, usage of sandwiching materials can affect the air permeability, stretchability and the drapability of TENG structures which reduces the wearability.

2.4.1.2. Core-shell-structured TENG developments.

A conductive fiber/yarn core can be encapsulated by a triboelectric outer material to manufacture this type of TENGs. Single-electrode-mode yarn-based TENGs are mostly manufactured in core-shell-based developments. An array of techniques such as electrospinning, dip coating, ring spinning, and braiding have been used to fabricate core-shell-structured TENGs**.** For example, Ma et al. manufactured a core-shell-structured, ultralight, nano-microfiber, hybrid single-electrode triboelectric yarns (SETY) with a diameter of 350 μm (Figure 2.5(a)), using the electrospinning technique [68]. This SETY was made of polyvinylidene fluoride (PVDF) and polyacrylonitrile (PAN) hybrid nanofibers as the shell and a conductive silver yarn as the core. This single-electrode TENG surface acted as the negative triboelectric layer when in contacted with human skin and the silver yarn was the electrode. The authors found that a PAN/ PVDF composition of 1:3 produced the best outputs. Maximum

instantaneous voltage, current density and charge density reached 40.8 V, 0.705 μA cm^{-2} and 9.513 nC cm^{-2}, respectively, under a 2.5 Hz movement. The instantaneous output power achieved a peak value of 336.2 μW when the external load resistance was 500 MΩ. This TENG was used to identify common fabric types (viscose fabric, polyester and polyurethane blend fabric, cotton fabrics, polyester fabrics, nylon fabric, and silk fabric) based on the electron affinity differences. Additionally, a glove was manufactured to identify hand gestures. Finally, this SETY was woven into an 8×8 pixel sensing fabric which was used for tactile sensing of smart textiles.

Dip coating is another technique that has been used to produce core-shell-structured TENGs. This technique is often used in the textile finishing process as a method of depositing uniform and thin layers of material onto fabrics [69]. Using a combination of dip coating and encapsulation, a stretchable and highly flexible coaxial structured, fiber-shaped triboelectric nanogenerator (F-TENG) has been manufactured (Figure 2.5(b)). Herein, silver nanowires (Ag NWs) and carbon nanotubes (CNTs) were deposited by dip coating to act as the electrode materials. Encapsulated polydimethylsiloxane (PDMS) was applied to the conductive fiber through brushing [70]. This F-TENG functioned in the single-electrode mode, employing a copper film as the counter triboelectric surface. It produced V_{OC} of 22 V, Q_{SC} of 7.5 nC, and I_{SC} of 0.6 μA at a tapping frequency of 5 Hz. The peak power density of this triboelectric yarn device, measured at a 1 Hz frequency, was 21.5 μW m^{-1} through an external resistance of 150 MΩ. The F-TENG was used as a tactile sensor. When the tapping force was less than 4 kPa, it provided a sensitivity of 5.2 mV Pa^{-1}; when the force was greater than 4 kPa, the sensitivity was 0.39 mV Pa^{-1}. Using this TENG, a self-powered motion detector was developed and sewn under a sock to identify different movements of the wearer.

Braiding is one of the oldest yet robust textile crafting techniques which is currently used to manufacture cords, strands, and 3D-braids [71]. This technology has also been used to manufacture core-shell-structured TENGs. A shape-adoptable, washable, and highly flexible TENG was manufactured via a three-dimensional five-directional braided (3DB) structure (Figure 2.5(c)), which was employed for biomechanical energy harvesting and multifunctional pressure sensing [72]. As the electrode of the

TENG, a silver-plated nylon yarn was used, which was covered uniformly with a polydimethylsiloxane (PDMS) coating. The peak power density of the PDMS-coated yarn (2 mm diameter) was 150 μW m^{-1} across an external load of 2 GΩ, under a frequency of 3 Hz. This yarn was converted into the 3DB-TENG through a four-step rectangular braiding technology and was operated in the vertical contact-separation mode. Under a compression load of 20 N at a frequency of 3 Hz, the 3DB TENG was able to produce V_{OC} and Q_{SC} of 90 V and 25 nC, respectively, and maximum power density of 26 W m^{-3}. A one-month-cycled test was conducted (more than 3 hours per day at 3 Hz motion frequency under 20 N loading) to check the durability of this device, with no significant reduction in electrical parameters. The 3DB-TENG has been used to fabricate an intelligent footwear system and a self-powered identity recognition carpet to investigate the feasibility of employing it in practical applications.

Compared to sandwiched fiber/ yarn-based structures, fabrication techniques used for core shell structured TENGs possess certain advantages in terms of scalability and wearability due to the usage of scalable textile fabrication techniques like braiding. However, the utilization of fabrication techniques such as electrospinning and coating techniques raise concerns regarding the durability of TENGs when it comes to applications in wearable sector since electro spun membranes and coatings tend to deteriorate when subjected to washing and abrading.

When analyzing fiber and yarn based TENGs, there are certain advantages such as being able to use fabrication techniques which can produce higher triboelectric properties such as electrospinning, electro spraying, and the ability to control material properties. However, the use of electrospinning, electro spraying and coating techniques for triboelectrically functionalization creates several major issues when it comes to the fabrication of wearable TENG devices. As mentioned above, electrospun membranes have poor mechanical properties. This increases the possibility of damaging triboelectric materials created from aforementioned techniques due to the forces applied on to wearable TENGs during day today activities of the wearer. This in turn reduces electrical and mechanical properties of TENG devices. On the other hand, coating techniques used for triboelectrically functionalizing yarns and fibers

reduces important properties such as flexibility and stretchability of yarns and fibers. This could reduce the comfort provided by textile materials and structures. Also, as mentioned previously, when coated surfaces are subjected to washing and other mechanical forces such as rubbing which textiles usually undergo, performance deteriorations can occur due to the removal of coatings. Finally, when it comes to mass production of fiber and yarn based TENGs, issues can arise due to higher production time and the higher cost due to the use of lab scale production techniques.

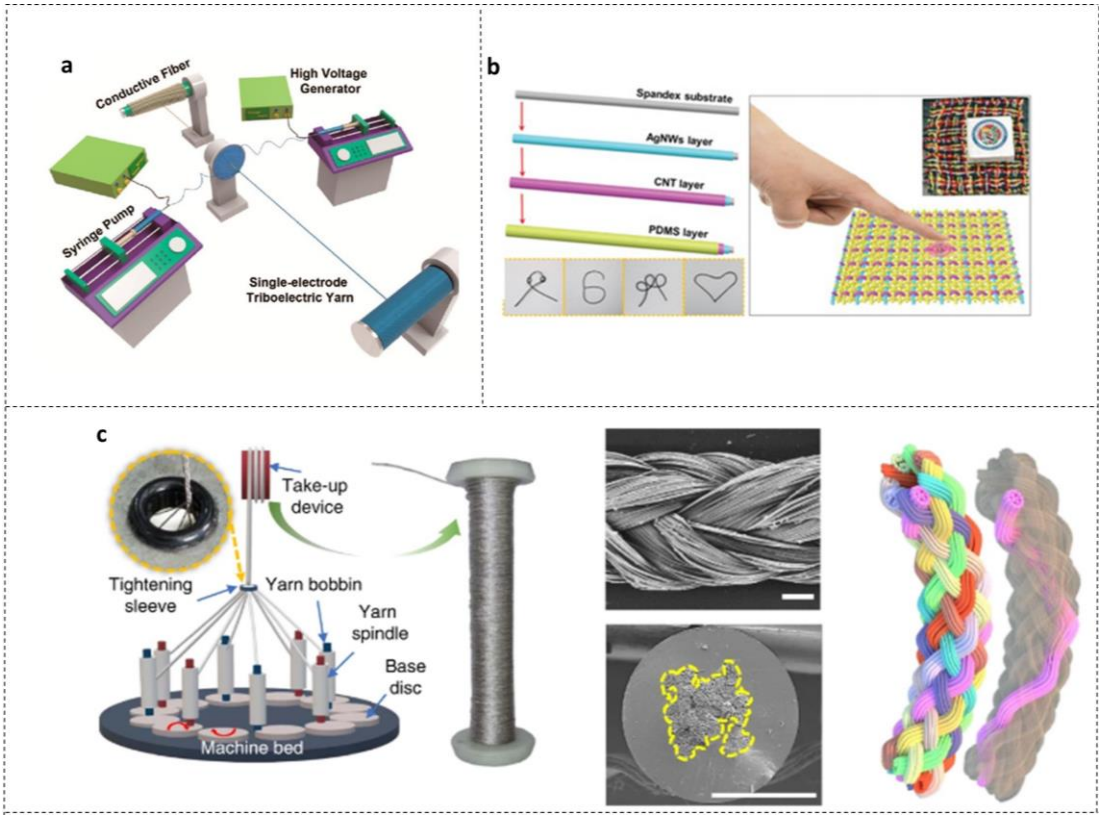

Figure 2.5: Core-shell-structured TENG developments. (a) Schematic illustration of the fabrication of SETY [68]. (b) Preparation and schematic images of F-TENG and a tactile sensor made of F-TENG [69]. (c) Schematic illustration of a multi-axial winding machine, the manufactured multi-axial winding yarn, and the surface morphology SEM image of a ten-axial winding yarn (scale bar: 200 μm) [72].

2.4.2. Fabric-based TENGs

Fabrics, with or without functionalization, have been increasingly used to develop textile TENGs. In comparison to fiber or yarn-based TENGs, fabric-based TENGs are easy to process and often exhibit better mechanical properties due to their structural

integrity and ease of processing. A multitude of textile manufacturing techniques such as knitting and weaving have been used to manufacture fabric-based TENGs. This section is focused on examining the fabric-based TENG developments dependent on the nature of triboelectric functionalization. Therefore, fabric-based TENGs are divided into surface-modified fabric TENGs and structurally-modified fabric TENGs. Moreover, structurally modified fabric TENGs are further segmented into knitted fabric TENGs and woven fabric TENGs, in order to better understand their development procedure and functional properties.

2.4.2.1. Surface-modified fabric-based TENG

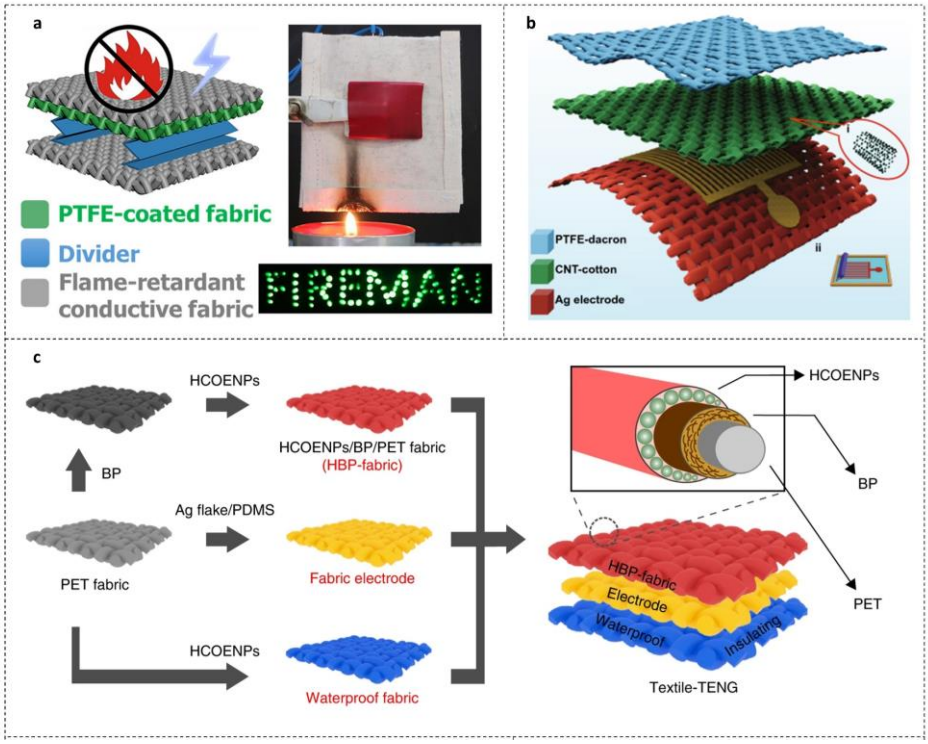

Figure 2.6: Surface-modified fabric-based TENG developments. (a) Schematic diagram of self-extinguishing flame-retardant TENG (FT-TENG) and photographs of FT-TENG showing the burning behavior [78]. (b) Schematic diagram of the F-TENG [79]. (c) Schematic illustration of the fabrication process of textile TENG based on PET fabrics [36].

In many of the fabric based TENG developments, the fabric has been used mainly as the substrate and then coated with triboelectrically functional materials. These types of TENGs predominantly contain surface modifications. A plethora of techniques have been used for such surface modifications in TENGs; for instance, layer by layer self-

assembly (LBL), [73] dip coating, [74], [75] electroless deposition, [76] chemical vapor deposition, [77] and screen printing [3].

In one example, the layer-by-layer self-assembly coating technique on cotton woven fabrics was utilized by Cheng et al. to manufacture a self-extinguishing, flame-retardant, textile-based TENG (Figure 2.6(a)) [78]. This TENG consisted of two flame-retardant silver fabrics, PTFE-coated cotton fabric, and a spacer. The flame-retardant coating was applied onto cotton fabrics via layer-by-layer self-assembly by alternatingly submerging cotton fabric in a cationic polyelectrolyte solution (polyethyleneimine and melamine) and in an anionic polyelectrolyte solution (phytic acid). Then, silver was coated onto the flame-retardant cotton fabric to fabricate the positive triboelectric material, as well as the electrode. To manufacture the negative triboelectric material, a cotton fabric was submerged in a PTFE dispersion liquid. A folded, spiring-like PTFE film was used as the spacer, which helped to connect (and separate) the two triboelectric surfaces. This TENG produced 343.19 mW m^{-2} power density output through a 700 MΩ resistor, subjected to a movement with 30 N compressive load at 3 Hz motion frequency. Furthermore, taking advantage of the flame retardancy, this TENG was used to construct a forest protection system and to illuminate LEDs worn by a firefighter via hand-tapping motion.

Using a combination of layer-by-layer self-assembly and screen printing, a self-powered wearable keyboard was fabricated (Figure 2.6(b)) as a SETENG [79]. Herein, two woven polyester cloths and a cotton cloth were used as substrates. A polyester cloth was coated with PTFE as the friction layer (negative triboelectric surface). The middle fabric layer was fabricated by layer-by-layer self-assembly of carbon nanotubes (CNTs) applied onto the cotton fabric. Moreover, a silver layer was screen-printed onto the polyester fabric to be used as the electrode of the TENG. The gradient porous structure of CNT@Ag fabrics provided the TENG with a large surface area, roughness, and elasticity, leading to a variation of contact resistance under applied pressure. The durability of this TENG was tested for 1000 cycles and no obvious deterioration of the I_{SC} was seen. The TENG was able to produce a I_{SC} of 170 μA m^{-2} and a peak power density of 3.8 mW m^{-2} through a 1 GΩ load, when subjected to a 1

Hz movement. Furthermore, this TENG was used to power a pedometer and a wearable keyboard.

Although applying a coating to triboelectrically functionalize a fabric surface is a scalable and relatively cost-effective method, continuous abrading against counter triboelectric surfaces and exposure to the environment might degrade the electrical performance of TENGs over time. Material encapsulation is a technique experimented to overcome these limitations associated with surface abrasion, and to improve the long-term reliability of TENGs.

Xiong et al. manufactured a durable skin-touch-triggered TENG using a synergetic triboelectric trapping layer consisting of black phosphorus (BP), encapsulated with cellulose-derived hydrophobic nanoparticles (HCOENPs) to reduce the degradation of the triboelectric material (Figure 2.6(c)) [36]. This TENG consisted of three polyethylene terephthalate (PET) knitted fabric layers. The foremost layer was dip-coated with BP and encapsulated with HCOENPs (triboelectric negative layer). The middle layer was the electrode of the TENG which was made by dip-coating the fabric with Ag flakes and PDMS. The bottom layer was dip-coated with HCOENPs, which was used to encapsulate the TENG electrode. Considering the electrical performance of the TENG, the device, which operated in the single-electrode mode, produced peak V_{oc} of 880 V, peak I_{sc} of 1.1 μA cm^{-2}, and peak power density output of 0.52 mW cm^{-2} through an external load of 100 MΩ, under a 4 Hz motion frequency and 5 N load (by voluntary tapping). The TENG also generated 60 V of voltage and 9 nC cm^{-2} of charge density under involuntary friction with the skin. As applications of this TENG, 150 LEDs were illuminated in series using gentle tapping (<5 N, 4 Hz), and a capacitor was charged to drive a digital watch.

As mentioned above, surface modifications to fabrics makes TENGs with better mechanical properties and improved scalability compared to fiber or yarn based TENGs due to the availability of well-established textile fabrication techniques which can be easily adopted for TENG fabrication. However, utilization of different coating techniques and printing techniques like dip coating, screen printing have been known

to compromise the wearable properties of the fabrics such as breathability and flexibility [80] which is a disadvantage in terms of the wearability.

2.4.2.2. Structurally modified woven fabric TENG developments

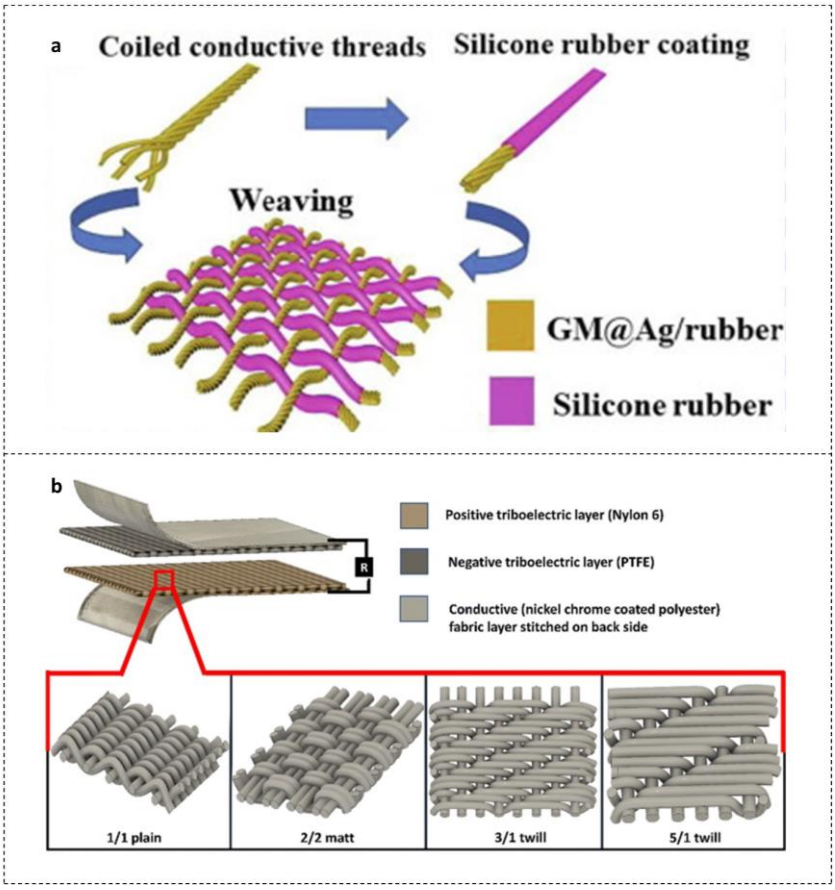

Figure 2.7: Structurally modified woven fabric based TENG developments. (a) Fabrication process of FSTTN [1]. (b) Schematic diagram of woven TENG and different woven samples used for the fabrication of the TENG units to monitor electrical performance [84].

Woven fabrics produced by interlacing two or more yarn sets. Recently, weaving has also been used for the fabrication of wearable TENGs due to superior wearability and multitude of design capabilities. Herein, recent developments in woven fabric TENGs will be discussed with a focus on the weaving process where the triboelectric functionalization has been introduced. This comprises both the use of different triboelectric materials for yarns and the weaving pattern changes.

Plain weave is the simplest form of woven structures. Plain-woven fabric TENGs have been developed for health monitoring, for instance, to monitor the bending angles of

the arm joint[1]. In this design, authors utilized a stretchable electrode to provide comfort to the wearer, which was fabricated using a mixture of silver-coated glass microspheres (GM@Ag) and solid rubber, deviating from the typical stretchable electrode manufacturing methods using silver nanowires [70], [81] or carbon nanotubes[1], [82], [83]. Thereafter, a fully stretchable textile based TENG (FSTTN) was manufactured (Figure 2.7(a)) by interlacing these coiled conductive yarns with silicone rubber yarns. During the fabrication, the electrode was made from a blend of GM@Ag and solid rubber at a 3:1 mass ratio and subsequent extrusion and vulcanization at 120 $^{\circ}$C. Five of the resulting conductive yarns were coiled to make an electrode (positive triboelectric layer). An identical electrode material was coated with silicone rubber to make the negative triboelectric layer. These yarns were woven using a traditional weaving method (plain weave) to complete the TENG. The resulting FSTTN durability was tested for 12000 cycles and no resultant increment in the electrode resistance was found. The electrical performance of the TENG was tested by flapping it with a piece of cotton fabric (freestanding triboelectric-layer mode), where a peak Voc of 138 V and a peak Isc of 2.1 µA were observed at 3 Hz under a 10 N force. The peak power output was 130 µW through a 120 MΩ load resistance, under the same excitation conditions. This TENG was employed to illuminate 50 LEDs and monitor bending angles of the arm joint.

Woven fabric manufacturing offers a variety of design capabilities with an array of weave patterns suitable for TENG designs. One such example is a study by Somkuwar et al. on woven fabric structures and their triboelectric outputs [84]. Herein, a VCSTENG was manufactured from nylon as the triboelectric positive material, and Teflon as the triboelectric negative material (Figure 2.7(b)). As the electrodes, a nickel-chrome plated thin polyester fabric was used. The layers were stitched together to connect the electrode, the conductive fabric, and the triboelectric layers. To study the effect of structural parameters on the electrical performance of this TENG, several 5 x 5 cm^2 woven fabrics with different structures (1/1 plain, 2/2 matt, 3/1 twill, 5/1 twill) were manufactured with 140tex yarns. By comparing the electrical outputs obtained from different structures, it was found that the 5/1 twill structure offered the best performance with a peak V_{OC} of 9.12 V, I_{SC} of 7.04 µA, and peak power density

of 12.84 μW cm^{-2}. The higher float length of the 5/1 twill structure, which increased the effective surface area of the TENG, was considered the main reason for these increased outputs. The authors fabricated a TENG device that could be placed under the foot using their woven fabric-based development.

Compared to surface modified woven fabric based TENGs, structurally modified woven TENG designs provide higher degree of wearability since they provide better air permeability: one of the major variables affecting the thermo-physiological comfort of textiles. When it comes to textile TENGs which use surface functionalization techniques such as applying different coatings, air permeability of the fabrics can be reduced due to the closing of micro pores in fabrics. On the other hand, structurally modified fabric based TENGs provide better scalability compared to TENG fabrics with surface functionalization, since there is a reduced need for post processing after manufacturing fabrics.

Even though structurally modified woven fabric TENGs provide certain advantages over surface modified woven fabric developments, woven fabric based TENGs possess certain disadvantages regarding wearability due to the lack of stretch. Stretchability of wearable TENGs is an important factor in determining the wearable performance and recent research have given more attention to the stretchability of TENGs [17][29], [34], [85]–[87].

However, knitted TENG has been known for their inherent stretch and comfort properties and good electrical performance. The following sections discuss wearable TENGs fabricated using knitting technology.

2.4.2.3. Structurally modified knitted fabric TENGs

Knitting is a major fabric manufacturing technique. Due to their interloped structure, knitted fabrics exhibit unique properties such as stretchability, breathability, and improved comfort to the wearer. A significant amount of knitted fabric related TENGs have been developed recently, which are broadly divided into weft knitted structures and warp knitted structures depending on their construction. Weft-knitted fabrics, which are further divided into single jersey (produced using a single set of needles) and double jersey (produced using two sets of needles), are more common in the textile

industry and these types of structures have been the predominant choice for the fabrication of fabric-based wearable TENGs. Herein, some of the most significant and recent knitted-TENG developments are discussed.

2.4.2.3.1. Single Jersey Knitted Fabric TENGs

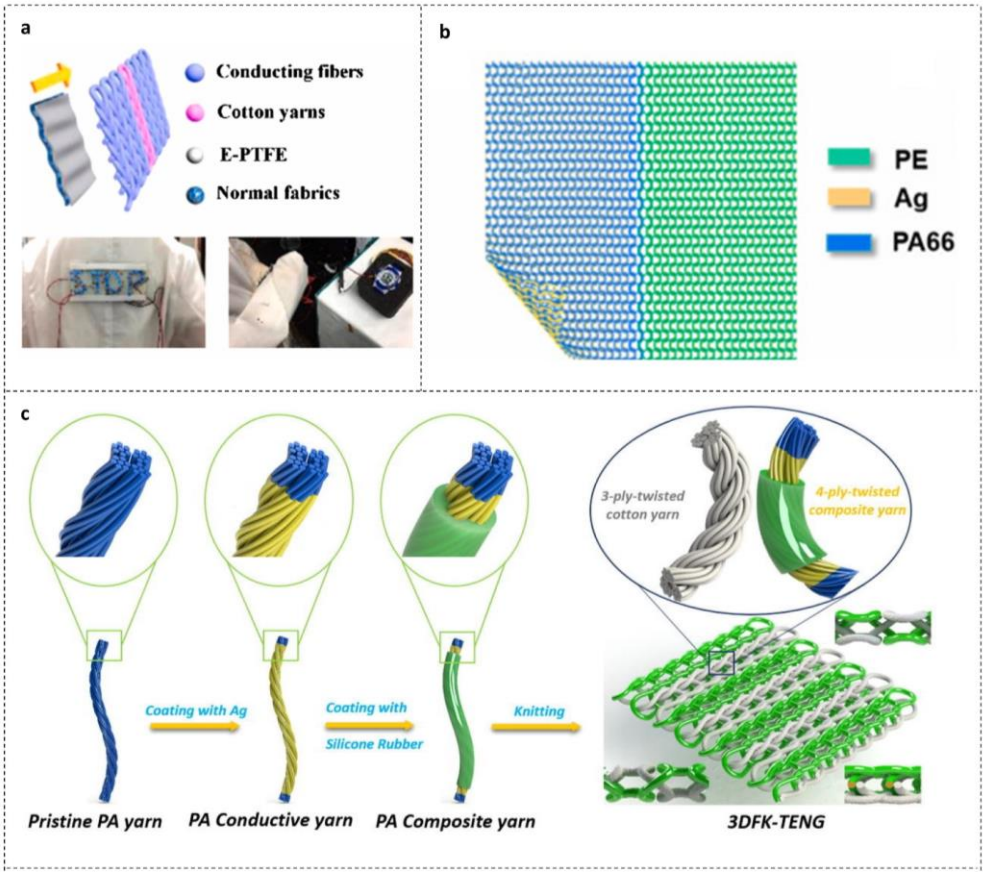

Figure 2.8: Knitted fabric-based triboelectric nanogenerators. (a) Schematic diagram of the laminated fabric, textile TENG and the self-powered warning indicator [85]. (b) The schematic illustration of the t-TENG [87]. (c) Manufacturing process of core-sheath yarn and 3DFIF-TENG [86].

Single jersey fabrics are knitted using a single bed of needles [88]. These fabrics are light in weight and high in porosity, hence provide good breathability which facilitates comfort to the wearer. However, single jersey fabrics tend to curl along the width of the fabric and have lesser dimensional stability.

Single jersey fabrics were used by Huang et al. to fabricate a freestanding-mode 2D TENG with a basic plain knit structure (Figure 2.8(a)) [85]. This design showed favorable characteristics for wearable applications such as air permeability, flexibility,

and washability. A silver-coated nylon yarn was used as both the positive triboelectric surface and the electrode. The triboelectric positive layer was divided into two parts (9x10 cm^2 each) by knitting a cotton yarn in between silver-coated nylon yarns. As the negative triboelectric surface, a PTFE membrane was fastened to a conventional polyester cloth using heat welding and a laminated fabric structure was manufactured. Sliding movement between the laminated fabric and the silver-coated fabric generated triboelectric charges for energy harvesting. The performance of different fabric textures was tested and the best design among these produced V_{OC} of 900 V, I_{SC} of 19 µA, and power density output of 203 mW m^{-2} through a load resistance of 80 MΩ. By comparing different fabric textures, it was found that TENGs with face loops (on the front side of the knitted fabric) provided better triboelectric outputs and higher stitch densities further improved electrical outputs. The suitability for wearable energy harvesting applications of this TENG was demonstrated by wearing it on the side of the waist (swinging motion). The TENG was able to power up a warning indicator, a digital watch, and a tracking and recognition setup to detect human motion.

Plating is used in knitting to produce desirable surface features, colored patterns, and to modify the wearable properties of the structure [88]. This technique was successfully used in developing single jersey knitted TENGs in which a conductive yarn and a dielectric yarn (Figure 2.8(b)) were used for the plating [87]. In this work, two types of TENGs were fabricated: (i) a coplanar sliding-mode TENG, and (ii) a VCSTENG. To fabricate the first TENG, silver-coated nylon yarns (electrode) were knitted underneath polyethylene (PE) yarns (negative triboelectric surface) and Nylon 6,6 yarns, respectively. Furthermore, a Nylon 6,6 fabric was used as the sliding material of this TENG. Under a 3 Hz motion frequency, this TENG was able to generate voltage of 120 V, current of 1.6 µA, and power density of 5.58 mW m^{-2} through a load of 70 MΩ. The VCSTENG was manufactured using PTFE as the negative triboelectric material and Nylon 6,6 as the positive triboelectric material. Both fabrics were plated with conductive silver electrodes. The effective contact area of the prepared TENG was 6.5 × 6.5 cm^2, which was tested under 30 mm separation at 3 Hz. The voltage obtained was 232 V, the current 6.8 µA, and the maximum power density 66.13 mW m^{-2} through an external load of 10 MΩ. To convert AC voltage into

DC and to improve energy conversion efficiency, a power management module (PMM) was connected to the TENG output, which was able to enhance the stored charge quantity and energy of a 15mF capacitor by 4 and 16 times, respectively, compared with the TENG without the PMM. In terms of applications, the TENG was used to successfully power up a calculator and an electronic watch.

2.4.2.3.2. Double jersey knitted fabric TENGs.

Unlike single jersey fabrics, two beds of needles are needed to produce double jersey fabrics [88], which increases yarn consumption. The fabrics produced in this method are heavier than the single jersey fabrics. On the contrary, knitting on two needle beds gives dimensional stability to the double jersey fabrics. Some of the most common double jersey fabric structures include rib and interlock knitted structures, which have been used to fabricate double jersey fabric-based knitted TENGs.

For example, Chen et al. developed a 3D double-faced interlock fabric-based TENG (3DFIF-TENG) (Figure 2.8(c)) using a flatbed knitting machine [86], which can be used as a flexible, substrate-free, wearable 3D tactile sensor. Here, cotton yarn was used as the positive triboelectric material. Additionally, a composite yarn, fabricated using a four-ply twisted nylon 6, 6 yarn and coated with silver and silicone rubber, was used as both the electrode and the negative triboelectric material. This TENG was fabricated as a plain interlock fabric that operates in the single-electrode mode. Due to the fabric structure, each cotton yarn loop was inserted immediately behind the nylon composite yarn; hence, any contact-separation movement (bending, stretching, etc.) of the fabric TENG could generate an alternating current. This fabric TENG exhibited desirable wearable characteristics such as flexibility, air permeability, and stretchability. The peak power density of the TENG was 3.4 mW m^{-2} through a load of 200 MΩ, and the device showed good linear co-relation between pressure and V_{OC}, I_{SC} and Q_{SC} in the range of 0.44 kPa. It was found that when the elongation of TENG was increased from 33% to 300% in a bend-stretch cycle, the V_{OC} and Q_{SC} had increased from 0.4 to 8 V and from 0.22 to 2.52 nC, respectively. Utilizing this capability, the TENG was used as a bend-stretch motion detector for robots and

humans. Furthermore, due to its pressure sensing ability, the TENG was used as a hand pressure sensor and a weighing cushion sensor.

As knitted fabrics provide superior electrical performance and wearable properties like stretchability, air permeability and flexibility, and variety of design capabilities, the fabrics have been used for many recent wearable TENG developments. Even though knitted fabrics provide TENGs with balanced electrical and wearable performances, one of their main drawbacks is the lack of knowledge on how knitting parameters relate with TENG electrical outputs. When considering woven fabric TENGs, research has been carried out to relate different woven fabric structures (e.g.: plain, twill, satin and sateen) and fabrication parameters affect the electrical performance of woven TENGs [84][89]. Even though different knitted fabric structures have been used for TENG fabrication (e.g.: single jersey, rib and interlock) the performance of each structure hasn't been comprehensively compared. Also, the effect of major knitting parameters like stitch length and yarn count on the electrical performance of TENGs hasn't been studied yet, which would be very useful for the growth of wearable knitted TENGs.

2.5. Summary of literature

The human body converts energy from food intake into several forms including chemical energy, thermal energy and mechanical energy. As an alternative to conventional power supplies, harvesting energy from the human body for wearable electronic devices has been widely researched. In this regard mechanical energy harvesting has been widely used via electromagnetic, piezoelectric, and triboelectric energy harvesting technologies. When comparing these three technologies, triboelectric energy harvesters possess several advantages such as high instantaneous outputs, working frequency tunable to be compatible with human motions (<10 Hz), simpler and less expensive construction. Triboelectric nanogenerators work on synergistic effects of contact electrification and electrostatic induction which occurs upon the contacting and separating of materials.

For the fabrication of wearable energy harvesters from TENG, several fabrication techniques have been used and textile technology is one of the leading technologies among them due to availability of highly performing triboelectric materials in textile

form, availability of well-established fabrication techniques, excellent wearable performances provided by textile structures and the ability to easily integrate triboelectric functionality during different stages of textile fabrication process.

Research has been carried out to integrate triboelectric functionality in different stages of textile fabrication process namely fiber manufacturing, yarn manufacturing, fabric manufacturing and fabric surface modification stages. When integrating triboelectric functionality, each of the above stages have advantages and disadvantages. Considering textile TENGs functionalized in fiber manufacturing stage, it allows the use of nanofiber fabrication techniques such as electrospinning for the fabrication process which makes superior electrical outputs. On the contrary, the use of electrospun fiber membranes reduces the mechanical strength of TENGs. Moreover, usage of lab scale fabrication techniques such as electrospinning reduces the scalability and efficiency of the TENG fabrication process. For fabricating TENGs functionalized in yarn manufacturing stage, coating techniques and electrospinning have been mainly used. Due to the usage of electrospinning higher outputs can be obtained from this method. As drawbacks, poor mechanical properties provided by electrospinning technique and inability of material coatings to withstand washing can be considered.

Fabric related TENG developments can be categorized into surface modifications and structural modifications. In considering the former, since fabric manufacturing techniques namely knitting and weaving are involved, better scalability of TENG fabrication process can be seen. Conversely, due to the use of electrospinning and coating techniques for surface modifications, issues similar to fiber and yarn based TENGs can be seen in fabric surface modified TENGs. Moreover, wearable properties of fabric structures such as air permeability, flexibility and hand feel can be deteriorated when different coatings are applied to fabrics.

Compared to yarn and fiber based TENGs and surface modified fabric based TENGs, structurally modified TENG architecture possess certain advantages such as improved scalability and better wearable performance. Structurally modified TENG developments can be mainly divided into woven fabric related developments and knitted fabric based developments. The former method has been frequently used for

wearable TENG fabrication since excellent wearable properties and the ability to produce superior electrical performances, and the effect of different woven structures and process parameters to triboelectric properties has been well studied. Even though woven fabrics possess wearable properties like air permeability and flexibility, the stretchability, which is essential for fabricating wearable TENGs, is lower for woven fabrics. This significantly limits the effectiveness of woven TENGs to be used in efficient and long-term wearable TENG applications.

Knitted fabric based structural modifications have also been used for TENG developments. In contrast to structurally developed woven fabric based TENGs, knitted fabric developments provide a superior stretchability while maintaining other comfort properties like air permeability and flexibility.

Due to the superior wearable and electrical properties provided by structurally modified knitted TENGs, knitting technology has been used in multitude of studies for fabricating wearable TENG devices. However, one of the main drawbacks in using knitting technology for wearable TENG development is the lack of knowledge between the effect of different knitted structures and knitting parameters on the electrical output performances.

CHAPTER 3

RESEARCH AIMS AND OBJECTIVES.

3.1. Research aim

This research aims to develop a novel standalone triboelectric nanogenerator using knitting technology, which has the potential to be used as a sensor for IoT applications.

3.2. Objectives

• Investigate the compatibility of selected textile materials/ polymers in developing knitted TENG architectures

• Evaluate the effect of different knitting parameters and knitted structures on triboelectric properties.

• Develop a high performing textile TENG architecture for wearable applications, and characterize wearable and electrical performances

CHAPTER 4
RESEARCH METHODOLOGY

A literature survey was carried out to gather previous knowledge on wearable TENGs, by focusing on textile based triboelectric nanogenerators. Several high performing materials were identified from this survey and considering the availability of materials and fabrication facilities, the material types and fabrication methods were selected. The effect of changing the process parameters and different structures of the selected fabrication technique (knitting) on the electrical performance of TENGs was evaluated. As the next step, based on the results of the aforementioned tests and considering the fabrication feasibility, a textile based TENG sensing device was developed which has the potential to be used in IoT applications, and the electrical and wearable performance of this device was evaluated.

4.1. Investigating the compatibility of selected textile materials/polymers in developing knitted TENG architectures.

As mentioned in the literature review, one of the major benefits in using textile substrates for TENG fabrication is the presence of highly triboelectrically chargeable textile materials in the triboelectric series. In relation to knitted TENG fabrication, the knittability of selected materials is also an important factor in material selection. To be knitted, the fundamental requirement is that the material should be in the form of yarns. Aside from that, other requirements are, appropriate yarn count compared to the gauge (number of needles per unit length) of the knitting machine and having appropriate surface roughness of the yarn. When selecting a material system for this research, firstly availability of the material in yarn form was considered. Thereafter the triboelectric performance of materials was considered through the literature survey. Finally, the knittability of the selected materials were considered by knitting a plain single jersey fabric, which is the most primary knit fabric design, using a gauge 10 Shima-Seiki SES122-S double bed computerized knitting machine available at the University.

To investigate the compatibility of textile materials, common textile materials available in yarn form were selected. Nylon 66 is in the topmost portion of the

triboelectric series and was used in previous research on TENGs in numerous occasions as a positive triboelectric material [3], [17], [86] and it has shown superior triboelectric properties. Also, nylon 66 possesses higher positive triboelectric properties compared to other common textile materials. So, nylon 66 was selected for this study. polyurethane (PU) is another material which occupies the positive portion of the triboelectric series. Recent research reported obtaining balanced wearable and electrical properties using knitting technique, where PU has been used as a triboelectric material with silicon based compounds, achieving excellent electrical outputs [80]. Hence for this study, a PU coated silver yarn was also tested as a positive triboelectric surface.

In view of the negative triboelectric materials, ample research on textile triboelectric nanogenerators has been done using Teflon: one of the most negative triboelectric materials, and obtained high electrical outputs [17], [84][86]. So, Teflon was also tested for this study. Furthermore, silver yarns were used as a potential material to act as both the electrode and a triboelectric material. Here, the silver yarn has been fabricated by coating nylon yarn with silver particles similar to some studies in literature [72][85].

Apart from above textile materials, polyethylene, polypropylene and PET (polyethylene terephthalate) yarns were available commercially, however, most of these available yarn types have been treated with antistatic agents in their fabrication process, which makes them unsuitable for this project as antistatic agents reduce triboelectrification. Also, the intrinsic properties of available yarns such as polyethylene (being in tape form) made them unsuitable for knitting due to low friction leading to lesser control of yarns.

Selected triboelectric materials were tested for knittability by knitting a single jersey fabric on SES-122S computerized knitting machine. From the selected materials, firstly nylon 66 yarn was tested, and nylon 66 yarn was knitted into a single jersey fabric without any major concerns (Figure 4.1(a)). When knitting the PU yarn, issues were raised due to the extreme stretchy nature of the PU yarn. When feeding the yarn to the knitting machine, the yarn had to move through a series of tension controlling

mechanisms. When feeding the PU yarn through these mechanisms, the yarn breakages occurred due to high stretch followed by necking. So, a fabric couldn't be knitted using the PU yarn. When knitting the Teflon yarn also, knittability issues occurred due to the form of the yarn. Teflon is a fancy yarn type and relatively low varieties were available. The available yarns were in tape form (single filament) with a smooth surface (Figure 4.1(b)). The smooth surface created uncontrollable slippages of the yarn when feeding to the knitting machine, leading to tangling of yarn followed by yarn, and knitting needle breakages. Finally, silver yarn was knitted. Even though surface of the silver yarn was rough, which created high tensions, a single jersey fabric was knitted without major issue (Figure 4.1(c)). So, finally considering knittability of yarns, nylon 66 was selected as the positive triboelectric material and silver was selected as the negative triboelectric material (and the electrode) in fabricating the sensing device.

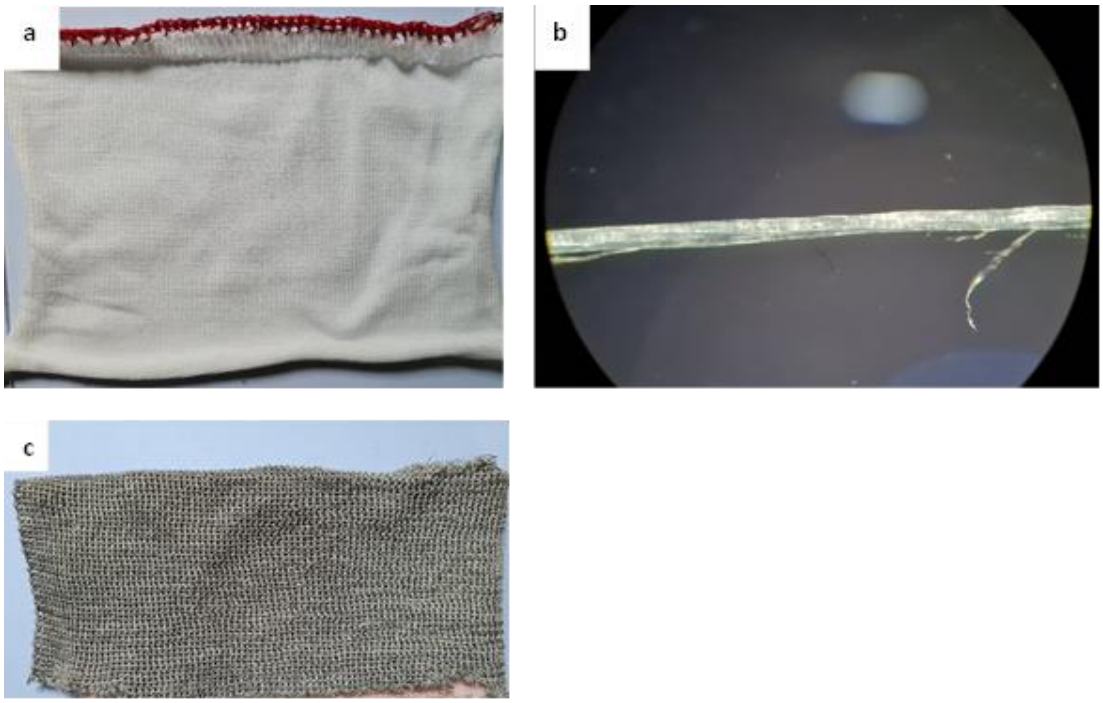

Figure 4.1: Material selection (a) Single jersey fabric knitted from nylon 66 yarn. (b) Microscopic image of Teflon yarn. (c) Single jersey fabric knitted from silver yarn.

4.2. Evaluating the effect of different knitting parameters and knitted structures on triboelectric properties.

Application of knitting technology for TENG fabrication can be seen frequently as mentioned in the literature review section. However, a comprehensive evaluation regarding the effects of different knitted structures and knitting parameters on triboelectric properties is lacking in the literature. So, this study was done to analyze the aforementioned relationship.

4.2.1. Selection of structures and knitting parameters for studying the effect on triboelectric energy harvesting

As reference to the literature review there are main two variations of knitted fabrics: single jersey and double jersey. The double jersey structures are divided into rib and interlock structures. Following this categorization, two sets of samples were fabricated as follows.

Table 4.1: Knitted structures changed for experiments.

Sample set	**Fabric structure**	**Controlled parameter & value**
Sample set 1	Single jersey	Loop length: - 36mm Yarn count: - 500dtex
	Rib	
	Interlock	
Sample set 2	Single jersey	Stitch density: - 323 Yarn count: - 500dtex
	Rib	
	Interlock	

.

To evaluate the effect of different knitted parameters on triboelectric charging, two parameters of single jersey fabrics were selected: stitch length and yarn count. Stitch length was selected for the study because it affects the dimensions of knitted fabrics and important fabric parameters such as wales per inch, courses per inch and areal density are dependent on the stitch length. The yarn count was selected as the next parameter since it affects the thickness of knitted fabrics which in turn affects the triboelectric charging as mentioned in the literature review section. Moreover, yarn count and stitch length determine the tightness or cover of the knitted fabrics which affects the triboelectric charging due to the variations in the effective surface area. Considering the above, the following sample sets were fabricated.

Table 4.2: Knitting parameters changed for experiments.

Fabric structure	**Fabric parameter**	**Values**	**Constant Parameters**
Single jersey	Loop length	30mm, 40mm, 50mm	Yarn count
Single jersey	Yarn count	350dtex, 700dtex, 1050dtex, 1400dtex	Loop length

4.2.2. Experimental method

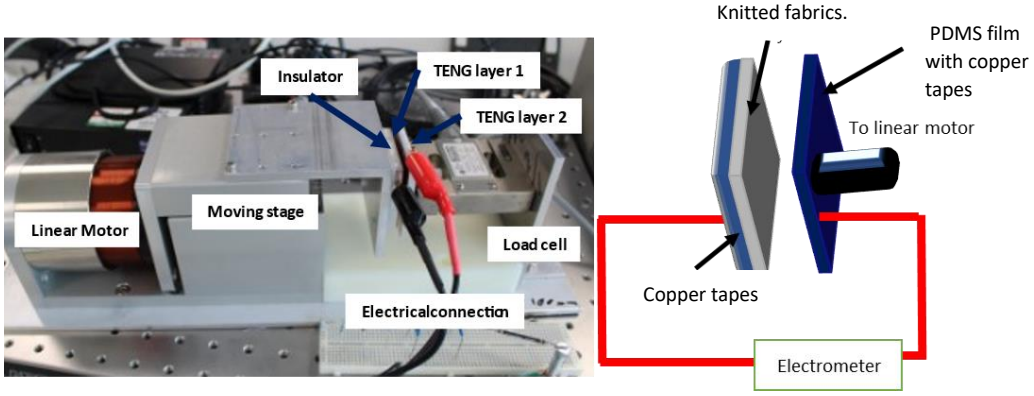

Figure 4.2: Electrical characterization setup.

Different knitted fabrics produced by changing knitted structures and knitting parameters were cut in to 5x5 cm^2 squares and attached to 5x5 cm^2 adhesive copper tapes and prepared positive triboelectric surfaces. Negative triboelectric surfaces were prepared by cutting 5x5 cm^2 square pieces of a PDMS film and attaching to 5x5 cm^2 square conductive copper tapes. For measuring electrical properties of each knitted fabric samples, positive and negative triboelectric surfaces were mounted on to the electrical characterization unit. The electrical characterization was done at the Wearable electronics laboratory, Loughborough University, UK (by Dr Ishara Dharmasena's group), using a characterization unit consists of a linear motor (Akribis AVM90-30) which can provide contact separation movements to attached triboelectric surfaces as depicted in figure 4.2. Negative triboelectric surface (TENG layer 1) was connected to a linear motor and the positive triboelectric layer (TENG layer 2) was mounted on to the load cell, which can measure the load applied to the triboelectric surfaces. Upon mounting the positive and negative triboelectric surfaces, their electrodes were connected to an electrometer via crocodile clips and conductive wires

to measure the electrical performance. Thereafter 1 Hz contact separation motions were applied at 10 N force by the linear motor with a 2 mm displacement. Charge (Q_{SC}), current (I_{SC}) and voltage (V_{OC}) outputs generated by the contact separation of TENG surfaces were recorded by a computer connected to the electrometer via LabVIEW software.

4.3. Developing high performing textile TENG architecture for wearable applications and characterizing their wearable and electrical performances.

The effect of different knitted structures and knitting parameters on triboelectric properties was evaluated (section 5.1) and based on the results obtained, a wearable knitted TENG sensor was developed which can sense stretch and tactile inputs. Thereafter the wearable performance of the fabricated TENG was evaluated.

4.3.1. Selecting a suitable TENG architecture

There are two main types of wearable TENG devices reported in literature. Attaching two triboelectric surfaces in different places (ex: - under arm and side of chest) in a way that two surfaces contact upon body movements is one method [90]. While this method produces simpler device structures, there are several drawbacks regarding the alignment of triboelectric layers, repeatability of outputs and the durability of outputs. Wearable TENG architectures with both the triboelectric surfaces together is the most widely fabricated wearable TENG architecture [29], [34], [86], [87] due to proper alignment of triboelectric pairs, durable and repeatable outputs and versatility. Considering the aforementioned advantage, latter architecture was used for the TENG sensor fabrication of this research.

4.3.2. Fabrication of wearable knitted TENG sensor

As mentioned in section 4.1, for producing the knitted fabric, sensor gauge 10 Shima-Seiki SES-122S double bed knitting machine was used. A schematic diagram of the TENG sensor fabric is given below (Figure 4.3).

Since the rib fabric exhibited the best electrical outputs from knitted structural variations (section 5.1.3), a rib fabric was chosen for crafting the sensor. Using the design capabilities of the knitting machine, a 3D rib fabric variation (a cell-type structure) which can contact and separate was constructed in the center of the fabric structure. This 3D structure was used as the triboelectrically active part of the TENG sensor fabric, and the 2D rib fabric structure was used to separate the cell without a charge leakage. As for the triboelectric materials, selected materials in 4.1 section were used: for the 3D rib variation of the bottom, a nylon 66 yarn was employed which is the positive triboelectric surface and silver-plated nylon yarn was used for the 3D rib variation of the top, which works as the negative triboelectric layer and the electrode material of the sensor. After knitting the sensing fabric, 2D rib fabric which is in the right and left hand sides of the sensing fabric was stitched together to form a tunnel-like structure, so that fingers can be inserted in to the aforementioned tunnel.

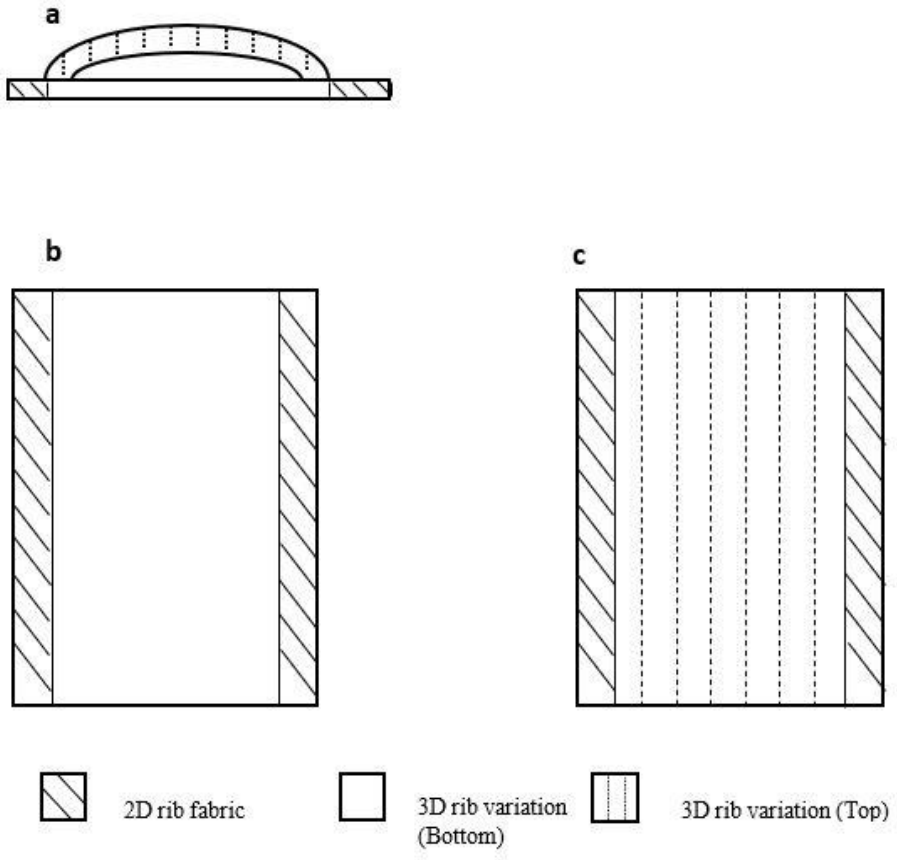

Figure 4.3: Schematic diagram of TENG sensor. (a) Side view. (b) Bottom view. (c) Top view

4.3.3. Working mechanism

This fabric operates in single electrode mode and emits electrical signals upon two types of motions: tapping (tactile) motions and stretching motions. When the 3D rib fabric variation at the top is tapped such that, it touches the 3D rib fabric at the bottom, triboelectrification occurs and the silver fabric (3D fabric at the top) gets a negative charge and nylon66 gets positively charged (3D fabric at the bottom). As the tapping force is removed from the silver fabric, it tends to separate from the nylon 66 fabric. This creates a negative potential on the silver surface. Since the silver surface is grounded through an electrode, net potential difference is created between the ground and the silver surface. Consequently, electrons move from the silver surface to the ground to negate the charge imbalance created by the negative charges on the silver surface. This creates a current from the ground to the silver surface through the electrode. When the silver surface is tapped again, a positive potential is induced onto the silver surface from the positive charges on the nylon surface. To negate the positive potential on the silver surface, electrons move from the ground to the silver surface through the electrode creating a current in the opposite direction (from silver surface to the ground). This way, an alternative current is generated upon the tapping motion on the sensor fabric.

Considering the electricity generation from stretching, as the sensor is stretched in the wale or course direction, the bottom nylon 66 fabric tends to stretch. Simultaneously the silver fabric, which is originally in the form of an arch, straightens and tends to contact with the bottom fabric. With the contact of the nylon 66, and silver materials, triboelectrification takes place. When the stretching force is released, two triboelectric surfaces separate, and a negative potential is induced on the silver surface. In the single electrode mode, since the electrode from the TENG is grounded, when the silver surface gets a negative charge, electrons flow to the ground from the silver surface through the electrode to neutralize the charge imbalance. Hence, a current circulation occurs from the ground to the silver surface. When separation of the triboelectric surfaces is reduced by applying a stretch to the fabric, the negative potential which was induced on the silver surface reduces. Hence a charge imbalance occurs again due to the lack of negative charges. To negate the charge imbalance, electrons move from

the ground to the silver surface creating a current flow in the opposite direction. In this manner an AC current is generated from a cell when the fabric is stretched and contracted.

4.3.4. Initial design and fabrication

In this section, initial development of the knitted TENG sensor is discussed.

4.3.4.1. Developing computerized fabric design and knitting the TENG fabric

To achieve the aforementioned functionality, a fabric design was developed using SDS-One KnitPaint (V 02 [64bit]) (Figure 4.4). After developing the design, a TENG sensor was knitted on a Shima Seiki SES122-S double bed knitting machine.

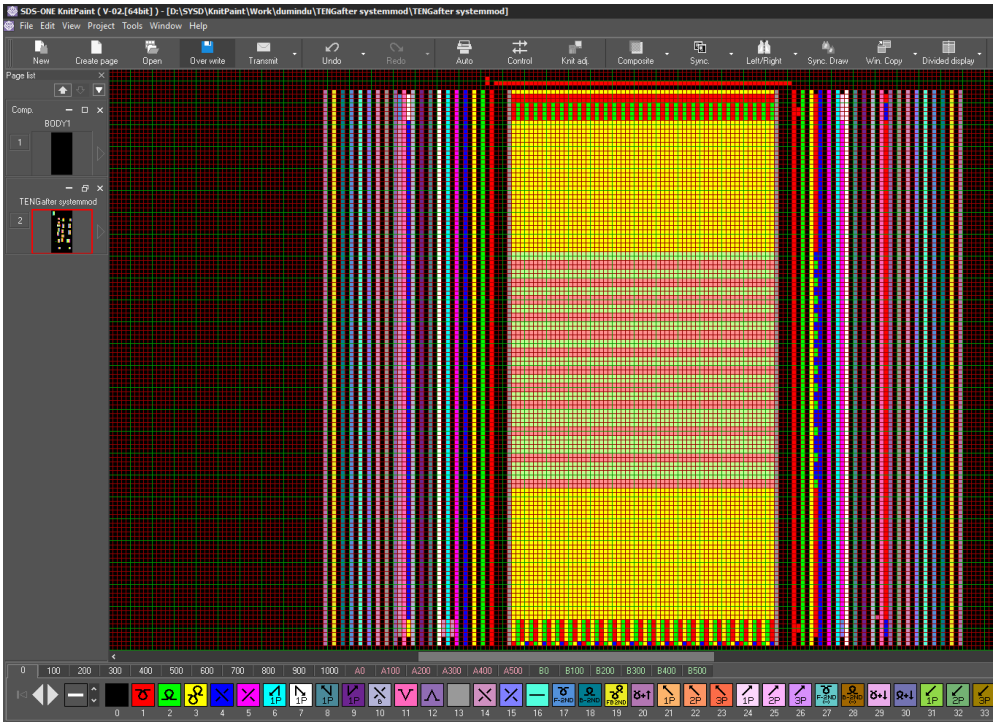

Figure 4.4: Programmed design of the knitted sensor fabric on SDS-One KnitPaint

4.3.4.2. Fabrication of sensing fabric for the initial design

From the 5th chapter, the effect of knitting parameters on TENG outputs was identified which can be increased through lowering the loop length and increasing the yarn count of knitted fabrics. When knitting the initial design, the loop length of the fabric was kept at 30mm, which is the lowest achievable loop length without thread breakages

and the yarn counts of the yarns were kept at high values. The materials and yarn counts used for the initial design are in table 4.3.

Table 4.3: Materials and yarn counts used for different parts of the sensing fabric in the initial design.

Part of the fabric	**Yarn type**	**Yarn count**
2D rib fabric	Nylon 66	1000 dtex
3D rib fabric (top) cell	Silver plated nylon	875 dtex
3D rib fabric (bottom) cell	Nylon 66	1050 dtex

4.3.4.3. Issues of the initial design

The following drawbacks were observed from the initial design.

1. Proper closing (contact) of the two 3D fabric layers couldn't be observed when stretches.
2. The arch shape structure (3D rib variation (top)) formed by the conductive fabric was slack and not uniform.

4.3.5. Final design and fabrication

In this section, issues occurred in the initial design was addressed and the final design was fabricated.

To have proper closing of two cells, firstly, the yarn counts of the bottom fabric of the cell was reduced from 1050 dtex to 700 dtex. From this modification, the cell of the fabric was able to close properly. To reduce the porous and hanging nature of the conductive fabric, the yarn count of the conductive yarn was increased. The yarn counts used for different sections of the final design are in table 4.5 and using these processing parameters fabrication of the knitted TENG sensor was done (Figure 4.5).

Table 4.4: Materials and yarn counts used for different parts of the sensing fabric in the final design.

Part of the fabric	**Yarn type**	**Yarn count**
2D rib fabric	Nylon 66	1000 dtex
3D rib fabric (top)	Silver plated nylon	1750 dtex
3D rib fabric (bottom)	Nylon 66	700 dtex

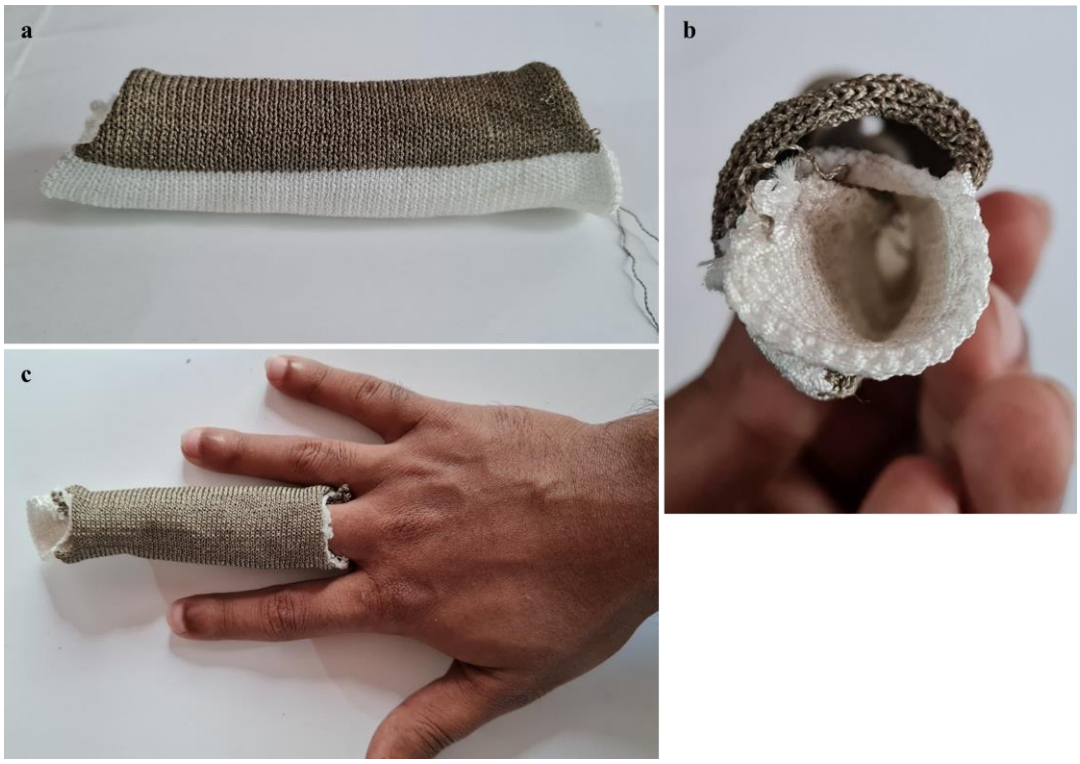

Figure 4.5: TENG sensor. (a) Top view. (b) Side view. (c) TENG sensor worn to a finger

4.3.6. Electrical performance characterization

Electrical performance of the fabric sensor was distinguished by measuring the electrical signals when the sensor was subjected to finger tapping, and measuring capability of identifying finger bending when the sensor is worn on to a finger.

4.3.6.1. Identifying finger tapping

The sensor was placed on a flat surface such that the conductive fabric faces upward direction. The electrode from conductive fabric was attached to an electrometer for measuring the electrical results. Thereafter, conductive fabric was tapped by finger such that the conductive fabric contacts with the nylon 66 fabric. The electrical signals generated by aforementioned movements were sent through the electrode coming from the conductive silver fabric to the electrometer for measuring.

4.3.6.2. Identifying finger bending

The TENG sensor was worn on the middle finger of the test subject and the electrode from the conductive fabric was connected to an electrometer to measure electrical

signals generated from the TENG. The TENG sensor mounted on index finger was bent in a distinctive pattern: 2 bends – pause – 1 bend – pause – 4 bends – pause – 3 bends – pause. Electrical signals generated from this bending pattern were collected through the electrode connected to the TENG sensor. The signals were measured through an electrometer.

4.3.6.3. Assessing the durability of conductive fabric

As mentioned in literature, one of the main issues in wearable TENGs is the lack of durability due to different surface modifications such as plating and coating. In this work, a silver-plated nylon yarn was used as a friction surface and an electrode, so, durability of silver-plated yarn was evaluated by measuring the resistance of the conductive fabric after washing and abrasion.

4.3.6.3.1. Resistance of conductive fabric after abrasion

A conductive fabric was knitted from silver-plated yarn using the same structure employed in the 3D fabric, on the top of the fabric. The fabric sample was kept in the room temperature for 24 hrs at 65% relative humidity for relaxation Thereafter, five fabric specimens were cut using a $10cm^2$ circular fabric cutter and four of them were mounted on holders used in Martindale abrasion tester. Mounted specimens were subjected to 2000, 4000, 6000 and 8000 abrasion cycles. Resistance of the abraded specimens were measured using a multimeter along a course of the fabric and compared with the resistance of the unabraded sample.

4.3.6.3.2. Resistance of conductive fabric after washing

A conductive fabric was knitted from silver-plated yarn, using the same structure employed in the 3D fabric on the top of the fabric. Then five of 4 x 10 cm^2 specimens were cut which weighed 4.5 g. For washing aforementioned fabrics, 5g/l phosphate reference detergent solutions were prepared. 270ml of washing solution was poured into sample washing canisters and one fabric specimen was put into a canister, so that the material to liquor ratio for washing is 1:30. Four such sample canisters were prepared, and the specimens were washed for 1, 2, 3 and 4 wash cycles (each of 30 min) while keeping 40 ^{0}C temperature in the sample washing machine. After washing,

the fabric samples were taken out and washed with distilled water and kept for drying for 24 hrs. After drying, the resistance of each fabric sample was measured along a course and compared with unwashed fabric sample.

4.3.7. Wearable performance characterization

For wearable performance characterization, comfort provided to the wearer was evaluated by testing air permeability (ISO 9237) because having multiple fabric layers in the sensing fabric can reduce the air permeability and the comfort. Since the area of the cell fabrics wasn't sufficient to carry out the test, the same fabric was knitted separately and used for the testing. The air permeability of a 2D rib fabric was measured and the air permeability of two 3D cells were evaluated together, and compared with the air permeability value of knitted TENG surface from a previous research [80].

Since the triboelectric surfaces are abraded frequently, abrasion resistance of the contact surfaces (conductive fabric and the nylon 66 fabric in the cell) was measured for 10000 cycles, using ISO 12947 standard.

CHAPTER 5
RESULTS AND DISCUSSION

5.1. Studying the effect of different knitting parameters and knitted structures on electrical performance of TENGs.

In this section, the experimental results on the impact of various knitting variables and knitted structures on the electrical properties of TENGs are discussed. For the experiments, the main knitting parameters selected were stitch length (loop length) and yarn count. As knitted structures, single jersey, rib and interlock structures were used.

5.1.1. Effect of stitch length on electrical performance

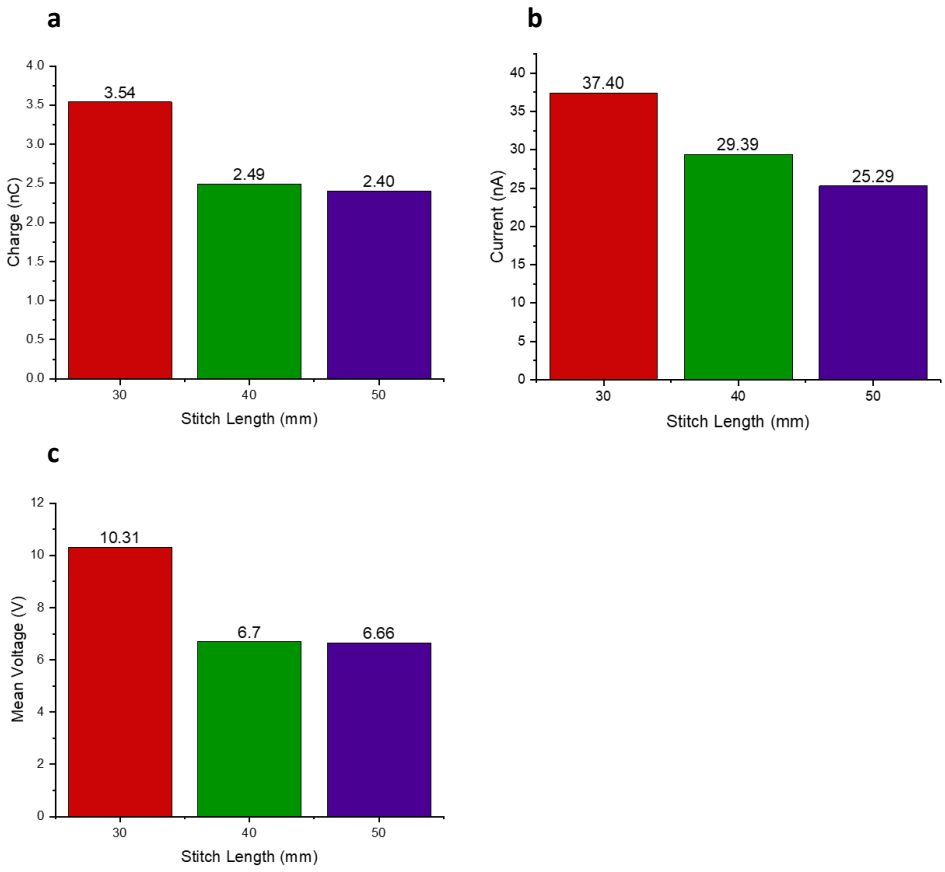

Figure 5.1: Effect of stitch length on electrical performance. (a) Q_{SC}. (b) I_{SC}. (c) V_{OC}

In this experiment, loop length of the knitted fabric samples were changed while keeping the yarn count as the controlled parameter. Here single jersey knitted fabric structures were used which were constructed by 500 dtex nylon 66 yarn. The short

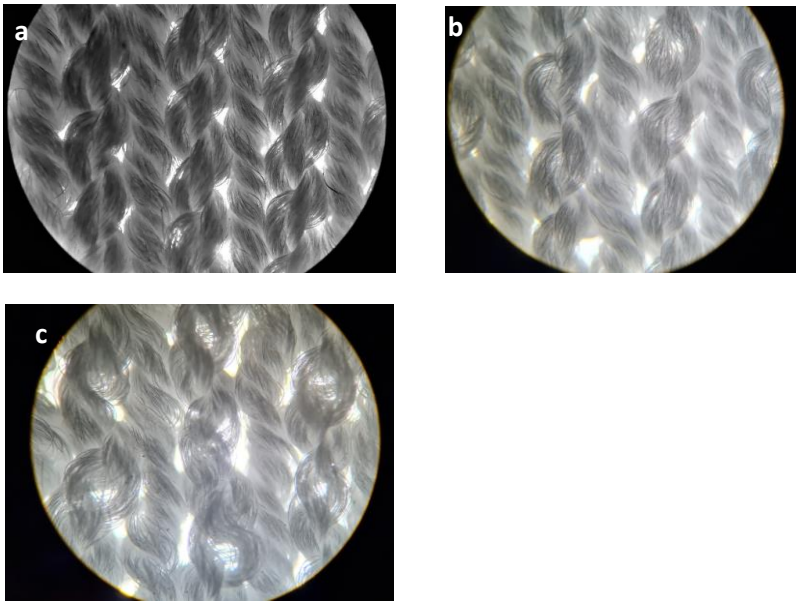

Figure 5.2: Microscopic images of knitted fabrics with (a) 30mm, (b) 40mm, (c) 50mm stitch lengths

circuit charge (Q_{SC}), short circuit current (I_{SC}) and open circuit voltage (V_{OC}) values of single jersey knitted fabrics with different loop lengths are in Figure 5.1. As shown in the graphs, when the loop length increased, the $V_{OC,}$ I_{SC} and Q_{SC} values were reduced. Microscopic images of knitted fabrics were taken (40 x magnification) (Figure 5.2) to examine the surface area covered by the fabric. From the microscopic images, it can be seen that the area covered by yarns in 30mm specimen is higher compared to 40 mm and 50 mm specimens and the 40mm and 50 mm specimens have nearly similar covers. Having higher surface coverage increases the area available for triboelectrification. Here, the 30mm specimen exhibited the maximum electrical output due to its high effective surface area. In electrical performance of 40mm and 50mm, 40mm sample has slightly higher outputs due to the marginally high surface area of 40mm sample. This behavior can be explained by the tightness factor which indicates the relative looseness or tightness of a single jersey knitted fabrics[88], calculated using the following equation.

$$TF = \frac{\sqrt{Tex}}{l} \qquad 5.1$$

Here, TF, represents the tightness factor of a single jersey knitted fabric and Tex and l are the yarn count of the fabric in Tex and the loop length of a loop in mm. The variations of the tightness factor calculated using equation 5.1 are depicted in figure 5.3. As shown in the figure 5.3, highest tightness is achieved by 30mm loop length sample which has the highest electrical outputs. 40mm and 50mm loop length samples exhibit reducing tightness which explains reducing electrical outputs in 40mm to 50mm samples respectively. Also, the tightness reduction between 50mm and 40mm

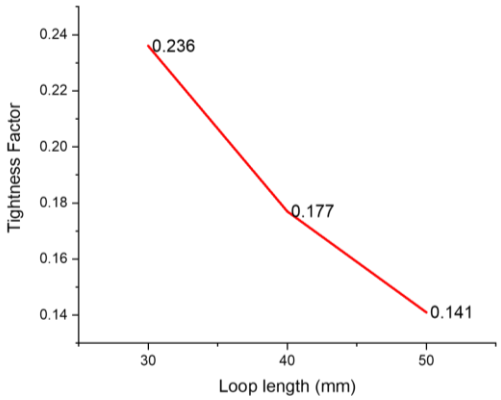

Figure 5.3: The variation of the tightness factor as a function of loop length (mm).

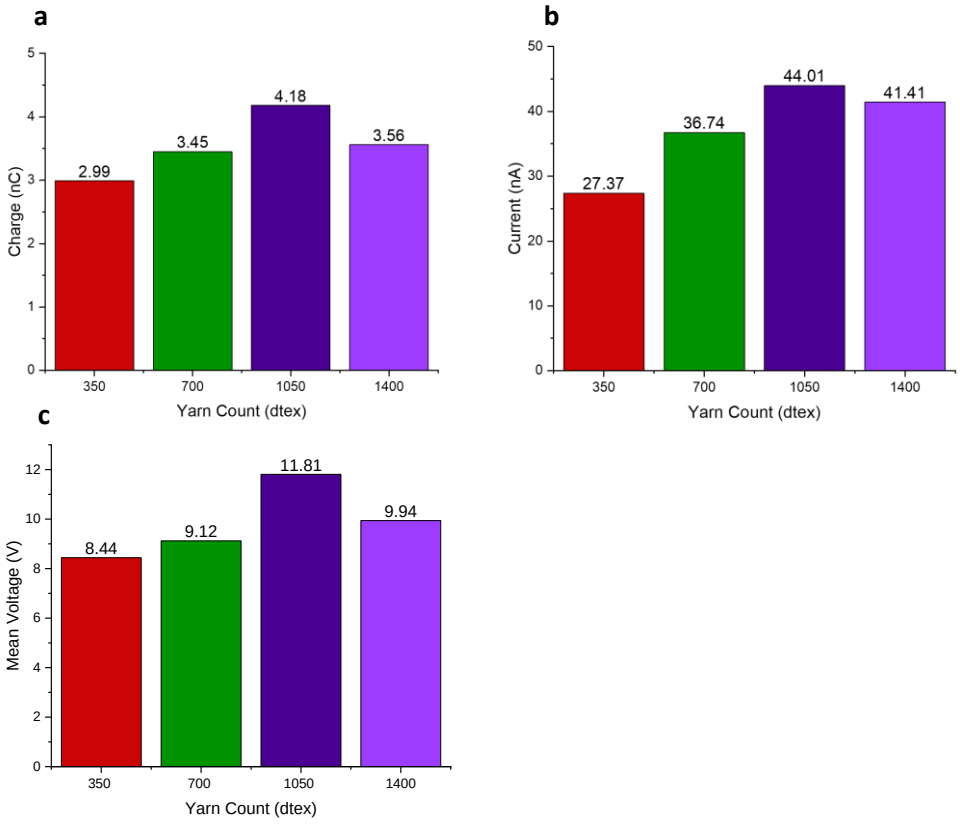

Figure 5.4: Effect of yarn count on electrical performance (a) Q_{SC}. (b) I_{SC}. (c) V_{OC}

samples is less than the tightness reduction of 30mm and 40mm samples, which explains the lesser electrical output reduction of from 40mm to 50mm samples compared to 30mm and 40mm samples.

5.1.2. Effect of yarn count on electrical performance

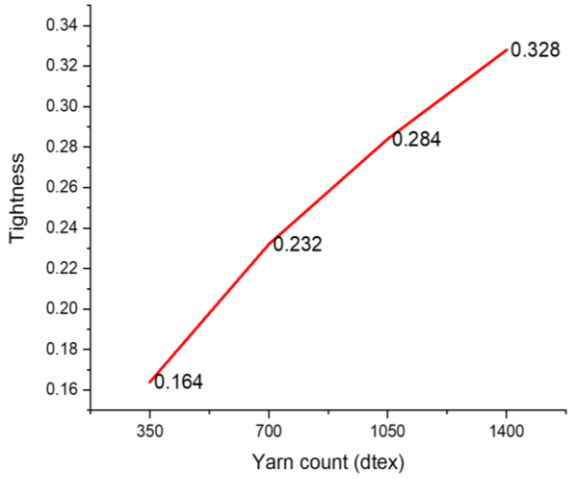

Figure 5.5: The variation of the tightness factor as a function of yarn count (dtex)

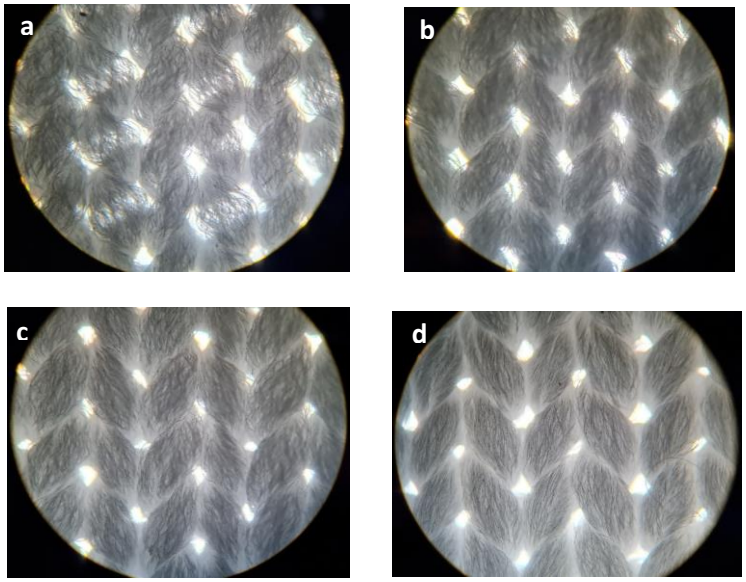

Figure 5.6: Microscopic images of knitted fabrics when the yarn count is increasing. (a) 350 dtex. (b) 700 dtex. (c) 1050 dtex. (d) 1400 dtex

The Q_{SC}, I_{SC} and V_{OC} values observed from the single jersey fabrics when the yarn count was changed are shown in Figure 5.4. Here, four yarn counts were used by plying four 350 dtex yarns while feeding to the knitting machine without twisting. Theoretically, when the yarn count is increasing, the tightness of knitted fabrics

increases [88] which signifies the fabric is more covered with yarn. This can also be seen in the graph, constructed from theoretically calculated values (Figure 5.5). In Figure 5.4, this trend can be seen up to 1050 dtex, but thereafter the electrical performance has been reduced. To explain this phenomenon, microscopic images of the above specimens were taken at 40x magnification. In the 5.6(a), 5.6(b) and 5.6(c) images, when the yarn count is increased, spaces between yarns are reduced. So, the electrical results should exhibit an increasing trend, which is evident in Figure 5.4 up to the 1050 dtex yarn. However, the electrical performances of 1400 dtex yarn exhibits lower values even though theoretical tightness factor values indicate an electrical performance increment due to the increment in tightness factor (Figure 5.5). This trend can be explained by the microscopic images. Compared to Figures 5.7(a) nylon filamens are tightly bound on to the yarn surface in Figure 5.7(b), probably due to the high tension created when using higher yarn counts. This reduces the surface area for triboelectrification, which causes electrical output reduction.

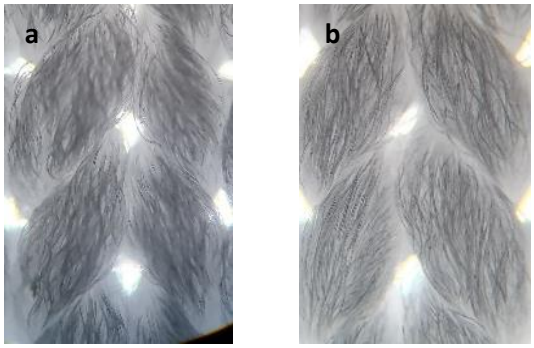

Figure 5.7: Magnified images of knitted fabrics from (a) 1050 dtex. (b) 1400 dtex yarns

5.1.3. Effect of different knitted structures on electrical performance

The effect of different knitted structures on the electrical performance was tested by producing knitting fabrics in two ways.

i. Knitting different structures by keeping the stitch density constant
ii. Knitting different structures by keeping the stitch length constant

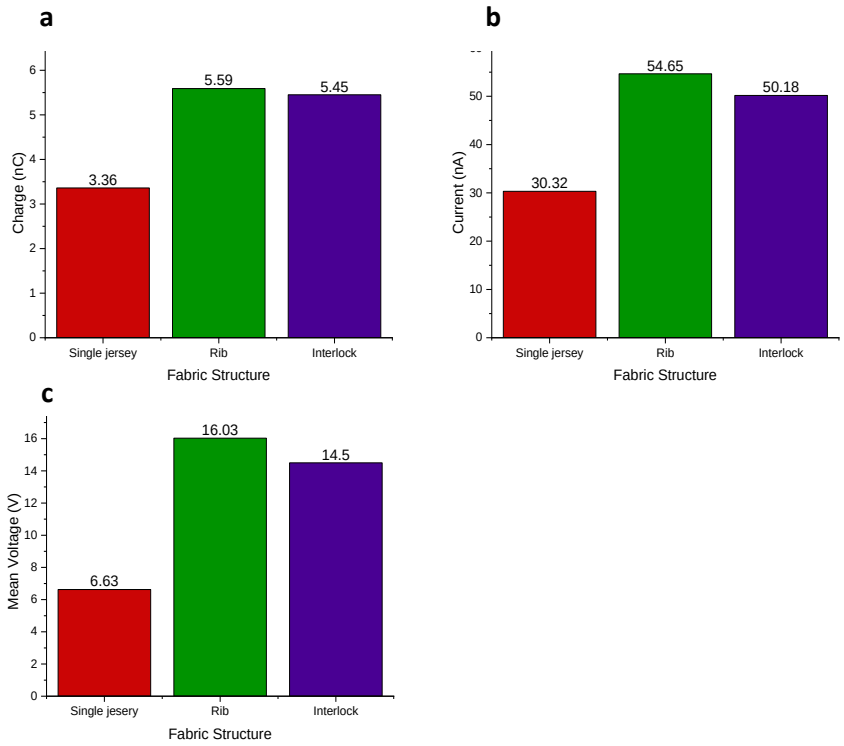

Figure 5.8: Effect of different knitted structures on electrical performance when stitch density is constant (a) Q_{SC}. (b) I_{SC}. (c) V_{OC}

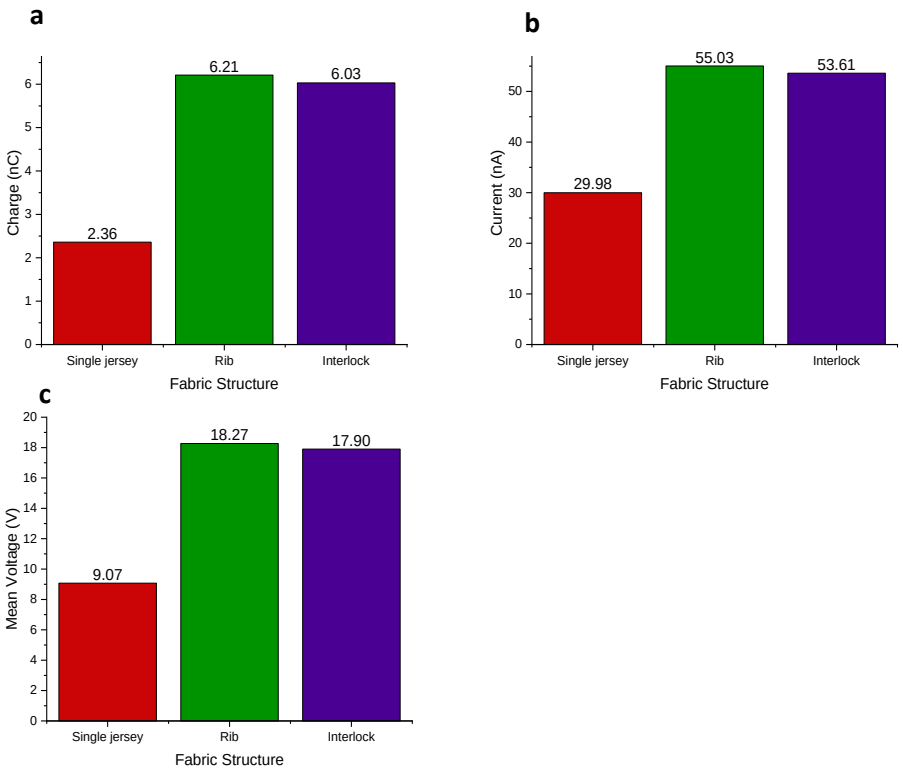

Figure 5.9: Effect of different knitted structures on electrical performance when stitch length is constant (a) Q_{SC}. (b) I_{SC}. (c) V_{OC}

When fabricating knitted structures with constant loop lengths, 36 mm was chosen and

as the stitch density, 323 stitches per square inch was chosen considering the feasibility of manufacturing. The electrical outputs for the aforementioned samples are shown in Figures 5.8 and 5.9.

In both scenarios, rib fabric showed the highest electrical outputs and interlock fabric showed the 2nd highest outputs, followed by single jersey structure. To explain these variations, only the microscopic images of each structure were taken (Figure 5.10, Figure 5.11), since tightness factor equation is only applicable for single jersey plain structures[88].

The single jersey fabrics showed the lowest electrical performance of all the structures. When studying the microscopic images, the lack of yarn cover in single jersey specimens can be clearly seen compared to rib and interlock structures. In fabricating double jersey structures (rib and interlock) which uses two needle beds for knitting, single jersey fabric structures need only one needle bed, so that the tightness of single jersey fabrics are less contrasted to double jersey fabrics, which is the cause for reduced electrical performance of single jersey fabrics. The lesser tightness of single jersey fabrics compared to rib and interlock fabrics can be also seen in microscopic

Figure 5.10: Microscopic images of (a) single jersey, (b) Interlock, (c) rib structures when stitch density is constant.

Figure 5.11: Microscopic images of (a) single jersey, (b) Interlock, (c) rib structures when loop length and yarn counts are constant.

images (Figure 5.10, 5.11). When comparing the microscopic images of rib and interlock fabrics, it is evident that the interlock fabric has a better cover compared to rib fabric, even though rib fabric exhibits higher electrical performance. Apart from the surface area of the triboelectric surface, thickness of triboelectric surfaces significantly contributes to the electrical performance of TENGs as mentioned in section 2.3.1. So, thickness of the above fabrics was measured in order to explain the slightly high electrical performance of rib structures (Figure 5.12).

In considering the graphs of the fabric thickness, it is apparent that the thickness of interlock fabric is approximately 35% higher than the rib fabric. So, having higher thickness of the interlock fabric can be assumed as a possible cause for the slight electrical output reduction of that fabric type. Apart from that, due to the needle formation of rib fabric (rib gating), they possess an ability to stretch well in the course direction compared to the needle formation of interlock fabrics (interlock gating) [88]. This stretchability enables the rib fabric to expand and move the loops which were formed in two beds into a single plane, when a stretch or compressive force is applied, thus increasing the fabric contact area. This phenomenon can possibly be a reason for the slightly higher outputs or rib fabrics since it increases the triboelectric contact area during the contact (and compression) of TENG surfaces. Even though calculating the tightness factor of different knitted structures might give better idea about the surface

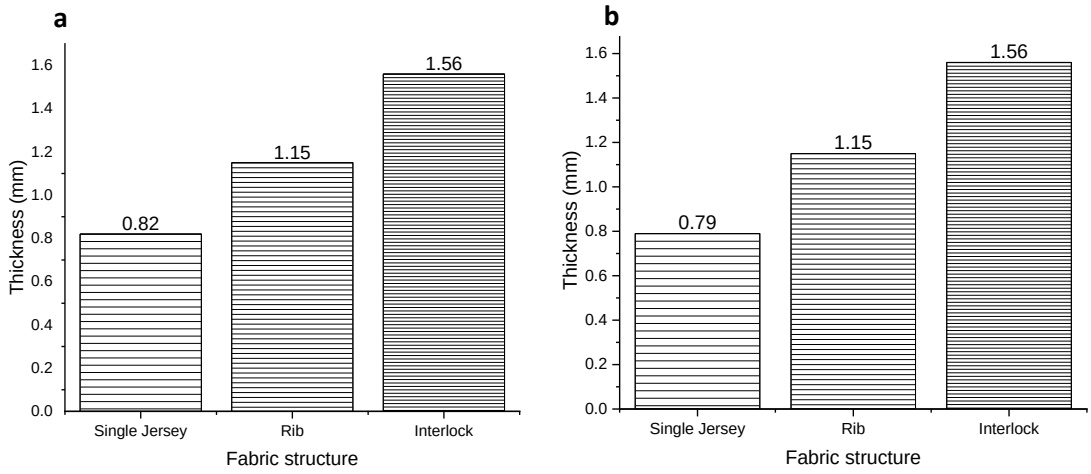

Figure 5.12: Thickness of different fabric structures (a) when stitch length is constant. (b) when stitch density is constant.

coverage. Here, different knitted structures weren't compared with each other since equation 5.1 can only be used to compare tightness factors of single jersey fabric structure [88].

5.2.Electrical characterization of knitted wearable TENG sensing device.

Electrical characterization of the TENG sensor was done by applying tapping and bending motions on the sensor, and following results were obtained during these tests.

5.2.1. Electrical performance of the sensing device under tapping motions

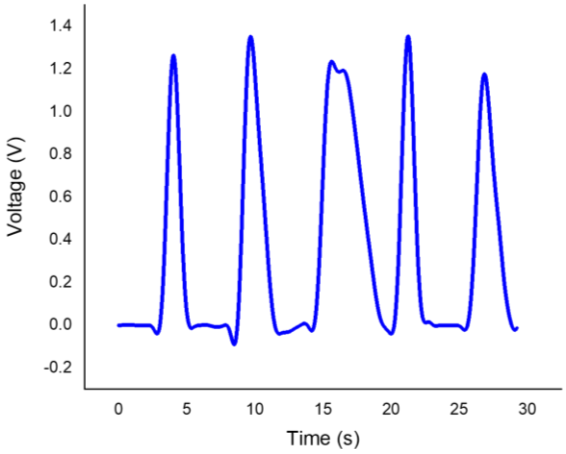

Figure 5.13: Electrical performance (V_{OC}) of knitted fabric sensor under tapping motion.

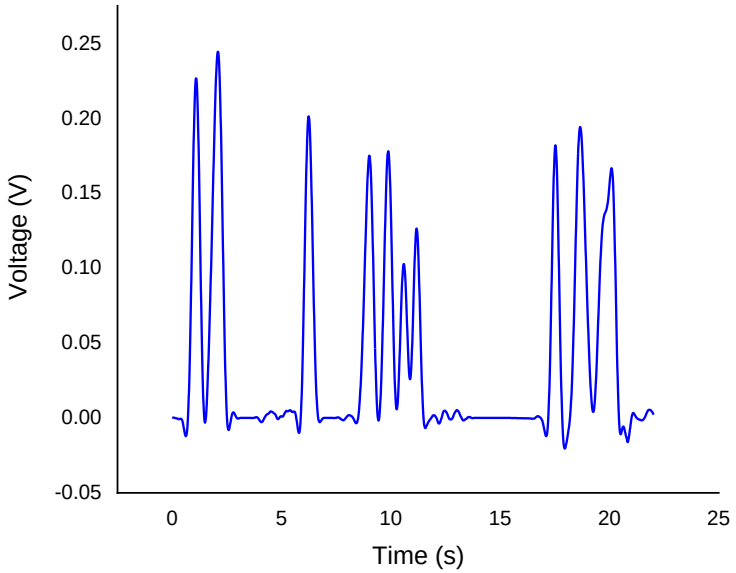

Figure 5.14: Voltage signals generated by TENG sensor on bending motions.

Figure 5.13 demonstrates the V_{OC} graph of the fabricated sensing device when it was subjected to five finger consecutive tapping movements from a finger. The differences of charge and voltage peaks can be attributed to the varying tapping forces applied to the TENG sensor.

5.2.2. Electrical performance of the sensing device under bending motions

TENG sensor was worn on a finger and the motion sequence specified in section 4.3.6.2 was applied. Following voltage signals were obtained from the TENG sensor upon providing bending motion sequence (Figure 5.14). As in the graph, the sensor was able to produce distinguishable voltage signals corresponding to the applied motion sequence. Compared to voltage signals generated from tapping motions, bending motion has generated comparatively lower voltage outputs, which can be assumed due to the lesser force, and contact generated by bending motions on triboelectric pairs, compared to tapping motions.

5.2.3. Assessing the durability of conductive fabric

The durability of the conductive fabric was assessed by measuring its resistance after abrasion and washing.

5.2.3.1.Durability of conductive fabric against abrasion

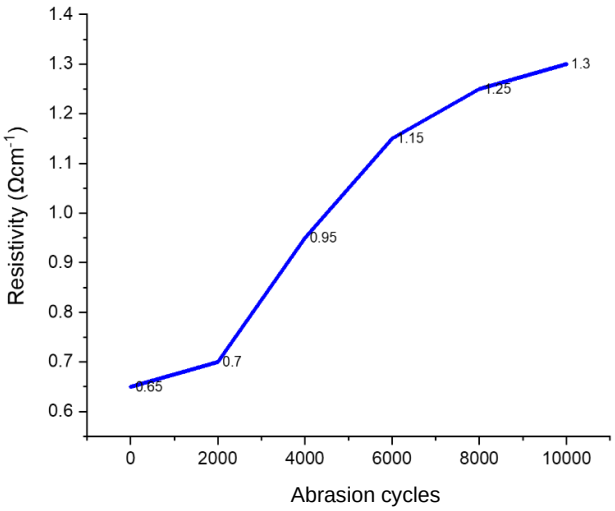

Figure 5.15: Resistivity of conductive fabric on abrasion

Resistance per unit length (resistivity) of the conductive fabric was measured according to the procedure mentioned in section 4.3.6.3.1. Conductive fabric was subjected to 10000 abrasion cycles. Following which, its resistivity only increased by 0.65 Ω cm^{-1} compared to the unabraded sample (Figure 5.15). The increment of the resistivity can be attributed to the removal of silver particles from the yarn. However, only a slight increment of resistivity after 10000 abrasion cycles ensures the durability of the conductive coating applied on the yarn and this also indicates the longevity of the TENG sensor when subjected to repeated usage.

5.2.3.2. Durability of conductive fabric against washing

The durability of conductive fabric against washing was measured according to procedure mentioned in section 4.3.6.3.2. The conductive cloth was subjected to four washing cycles and the resistance was measured along a course up to 10cm, at 2cm intervals (Figure 5.16). The resistance of the conductive fabric has increased during washing. However, after the first wash, the rate of increment in the resistance has reduced which indicates that after the initial removal, the reduction of conductive particles from the fabric is less during the subsequent washes. Also, a reduction of the resistance increment can be seen in the washed specimens with the increment of the length. Usually, knitted fabrics tend to shrink or relax after washing due to the

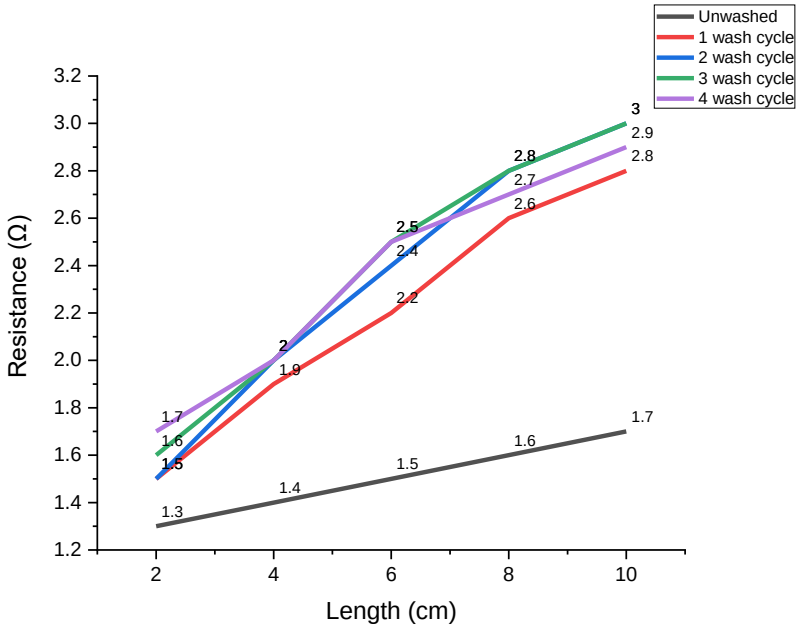

Figure 5.16: Resistance of conductive fabric on washing

reduction of tensions applied while knitting. The aforementioned reduction of the increment of resistance can be attributed to the relaxation of the conductive fabric, hence less actual length of yarn along a course. However, since the maximum increment of resistance along a course is minor as 1.3 Ω (4 wash cycles), it can be assumed that the resistance increments after washing is acceptable since TENGs are inherently high impedance devices (internal impedance typically in Giga-Ohm range).

5.3. Wearable performance characterization

The wearable performance of the TENG sensor was characterized by measuring air permeability and abrasion resistance of fabric components in the sensor.

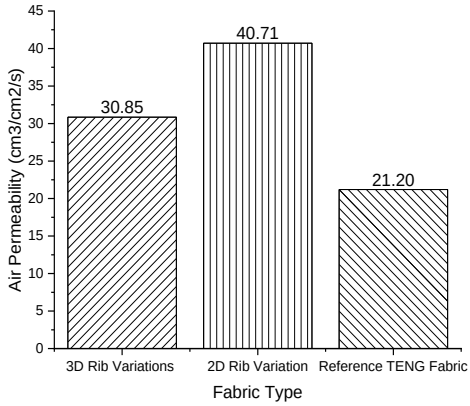

Figure 5.17: Air permeability of fabric structures of the knitted TENG sensor

5.3.1. Results of the air permeability test

The air permeability test was carried out as mentioned in section 4.3.7. The air permeability of 2D rib fabric was the highest (Figure 5.17) (40.71 $cm^3/ cm^2/ s$). 3D rib fabric variations were tested such that two fabrics in the cells are on top of each other, since the least air permeability occurs at that state. Even so, 3D rib fabric variations were able to exhibit adequate air permeability (30.85 $cm^3/ cm^2/ s$) compared to the reference TENG fabric (21.20 $cm^3/ cm^2/ s$) found in literature [80] proving superior wearable performance of this design.

5.3.2. Results of the abrasion test

An abrasion test was carried out for 3D rib fabrics. After 10000 abrasion cycles, no visible damage to threads of the tested fabric could be seen (Figure 5.18). This

demonstrated the durability of the TENG sensor for practical applications.

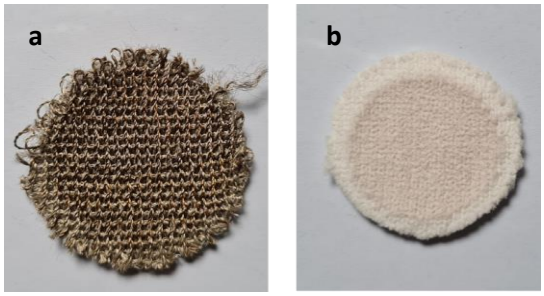

Figure 5.18: 3D rib fabrics after 10000 abrasion cycles. (a) conductive rib variation. (b) nylon 66 rib variation

CHAPTER 6

APPLICATIONS OF THE FABRICATED SENSOR

IoT can be defined as network of physical objects that are embedded with software, sensors and other technologies with the purpose of exchanging data with each devices and systems via internet [91]. With the current development of IoT, many novel applications have been realized such as smart homes, smart wearables, health, smart manufacturing and smart agriculture. The outcome of this research is related to the health sector. Currently the population above age 65 is growing at a higher speed compared to other age groups and the world health organization has revealed that the population above the age 60 will grow from 12% to 22% within 2015 to 2050. Moreover, it has been identified that roughly 80% of the older population have at least one chronic disease [92]. This increasing growth of older population will create higher medical needs and caretaking facilities and currently available facilities won't be sufficient in catering to these needs [92]. As a solution for this increasing demand for healthcare facilities, IoT based in home health monitoring applications have immerged [93], enabling in home disease prevention, diagnosis and lifestyle management.

One of the main areas in which IoT technology is being used in healthcare is rehabilitation. As an example, Alexandre et al have developed a smart glove which can be used for natural interactions with therapeutic serious games for upper limb rehabilitation [94]. The hand glove has been equipped with sensors, which were mounted on each of the fingers to detect flexes and forces applied by fingers. When a specifically design game was played by the user, which involves finger movements, the sensors attached to the gloves picked up signals corresponding to finger movements and was able to send acquired data to doctors for studying the medical condition of the user.

Since the wearable TENG sensor fabricated in this project has shown the ability to detect finger tapping and finger bending motions, it can be used for applications related to rehabilitation as mentioned above, by replacing commercially available sensors with the textile TENG sensors. Therefore, the textile TENGs developed in this study demonstrate excellent potential for future IoT applications.

CHAPTER 7

CONCLUSIONS

In this research, the effect of different knitted parameters and knitted structures on triboelectric properties were studied. Based on the findings, a knitted TENG sensor was developed which has the potential to be used for IoT applications, and the wearable and electrical performance of this TENG device were evaluated.

In the beginning of the research, suitable material system was selected for fabrication of knitted TENG device considering knittability of available materials, availability of materials in yarn form and relative position of the materials in the triboelectric series. Thereafter, different knitted structures: single jersey, rib and interlock were fabricated using the selected positive triboelectric material, while changing main knitting parameters: yarn count and stitch length. Subsequently, electrical properties of knitted fabrics were evaluated. From this study it was identified that the increment of stitch length has a negative effect on triboelectric properties and increment of yarn count has a positive effect on triboelectric properties, due to the surface area reduction provided by increment of loop length and surface area increment provided by increasing yarn count. Structure wise, rib fabrics produced the highest electrical outputs followed by interlock and single jersey structures. The cause for the high electrical performance was found to be the synergistic effect of increased surface area and lesser thickness of the rib fabrics.

Based on the results obtained, a wearable knitted TENG sensor was fabricated which can produce electrical signals upon tapping and bending of fingers. Electrical performance of the TENG sensor was evaluated by bending TENG worn finger in a distinctive pattern measuring output voltage values, and the sensor was able to produce voltage signals according to the finger bending pattern. Furthermore, durability of conductive materials used was evaluated by measuring the electrical resistance of the conductive materials after subjected to washing and abrasion and the conductive fabric was able to withstand four wash cycles and 10000 abrasion cycles without a significant increment of resistance. Furthermore, the wearable performance of TENG device was evaluated by measuring air permeability of different fabric layers of the knitted sensor

and testing the abrasion resistance of friction surfaces used. Measured air permeability of different fabric layers were compared with the air permeability values of recently fabricated TENG device and all the fabric layers of the knitted TENG sensor exhibited higher air permeability values indicating better comfort properties. Moreover, friction surfaces were able to withstand 10000 abrasion cycles without thread breakages. Finally, possibilities of using the knitted TENG sensor for IoT applications were explained by comparing recently developed wearable IoT devices.

The fabricated TENG sensing device was able to measure bending of a finger. This can be further developed in future by fabricating and attaching sensors to each of the fingers in hand, so that the movements of fingers when performing different activities can be compared. These sorts of developments will be extremely useful in application areas such as health monitoring, physiological sensing and in rehabilitation monitoring purposes.

REFERENCES

[1] K. R. S. D. Gunawardhana, N. D. Wanasekara, and R. D. I. G. Dharmasena, "Towards Truly Wearable Systems: Optimizing and Scaling Up Wearable Triboelectric Nanogenerators," *iScience*, vol. 23, no. 8, p. 101360, Aug. 2020, doi: 10.1016/J.ISCI.2020.101360.

[2] J. Li *et al.*, "Triboelectric nanogenerators enabled internet of things: A survey," *Intell. Converg. Networks*, vol. 1, no. 2, pp. 115–141, 2020.

[3] W. Paosangthong, R. Torah, and S. Beeby, "Recent progress on textile-based triboelectric nanogenerators," *Nano Energy*, vol. 55, no. August 2018, pp. 401–423, 2019, doi: 10.1016/j.nanoen.2018.10.036.

[4] S. Wang, L. Lin, and Z. L. Wang, "Triboelectric nanogenerators as self-powered active sensors," *Nano Energy*, vol. 11. 2015. doi: 10.1016/j.nanoen.2014.10.034.

[5] Z. L. Wang, "Triboelectric nanogenerators as new energy technology for self-powered systems and as active mechanical and chemical sensors," *ACS Nano*, vol. 7, no. 11. 2013. doi: 10.1021/nn404614z.

[6] A. J. Bandodkar and J. Wang, "Non-invasive wearable electrochemical sensors: A review," *Trends in Biotechnology*, vol. 32, no. 7. 2014. doi: 10.1016/j.tibtech.2014.04.005.

[7] M. Zhou, M. S. H. Al-Furjan, J. Zou, and W. Liu, "A review on heat and mechanical energy harvesting from human – Principles, prototypes and perspectives," *Renew. Sustain. Energy Rev.*, vol. 82, no. November 2017, pp. 3582–3609, 2018, doi: 10.1016/j.rser.2017.10.102.

[8] R. D. I. G. Dharmasena and S. R. P. Silva, "Towards optimized triboelectric nanogenerators," *Nano Energy*, vol. 62. Elsevier Ltd, pp. 530–549, Aug. 01, 2019. doi: 10.1016/j.nanoen.2019.05.057.

[9] T. E. Starner and J. A. Paradiso, "Human-generated power for mobile electronics," in *Low-Power Electronics Design*, CRC Press, 2004, pp. 45-1-

45–35. doi: 10.1201/9781420039559.ch45.

[10] S. A. Graham, B. Dudem, A. R. Mule, H. Patnam, and J. S. Yu, “Engineering squandered cotton into eco-benign microarchitectured triboelectric films for sustainable and highly efficient mechanical energy harvesting,” *Nano Energy*, vol. 61, no. February, pp. 505–516, 2019, doi: 10.1016/j.nanoen.2019.04.081.

[11] R. Riemer and A. Shapiro, “Biomechanical energy harvesting from human motion: theory, state of the art, design guidelines, and future directions,” *J. Neuroeng. Rehabil.*, vol. 8, no. 1, p. 22, 2011, doi: 10.1186/1743-0003-8-22.

[12] M. U. Anjum, A. Fida, I. Ahmad, and A. Iftikhar, “A broadband electromagnetic type energy harvester for smart sensor devices in biomedical applications,” *Sensors Actuators, A Phys.*, vol. 277, 2018, doi: 10.1016/j.sna.2018.05.001.

[13] J. Zhao and Z. You, “A shoe-embedded piezoelectric energy harvester for wearable sensors,” *Sensors (Switzerland)*, vol. 14, no. 7, 2014, doi: 10.3390/s140712497.

[14] M. O. Kim *et al.*, “Flexible and multi-directional piezoelectric energy harvester for self-powered human motion sensor,” *Smart Mater. Struct.*, vol. 27, no. 3, 2018, doi: 10.1088/1361-665X/aaa722.

[15] S. Niu and Z. L. Wang, “Theoretical systems of triboelectric nanogenerators,” *Nano Energy*, vol. 14, pp. 161–192, 2015, doi: 10.1016/j.nanoen.2014.11.034.

[16] F. R. Fan, Z. Q. Tian, and Z. Lin Wang, “Flexible triboelectric generator,” *Nano Energy*, vol. 1, no. 2, pp. 328–334, 2012, doi: 10.1016/j.nanoen.2012.01.004.

[17] D. G. Dassanayaka, T. M. Alves, N. D. Wanasekara, I. G. Dharmasena, and J. Ventura, “Recent Progresses in Wearable Triboelectric Nanogenerators,” *Adv. Funct. Mater.*, 2022, doi: 10.1002/adfm.202205438.

[18] Z. L. Wang, J. Chen, and L. Lin, “Progress in triboelectric nanogenerators as a new energy technology and self-powered sensors,” *Energy Environ. Sci.*, vol.

8, no. 8, pp. 2250–2282, 2015, doi: 10.1039/c5ee01532d.

[19] Y. Yang *et al.*, "Human skin based triboelectric nanogenerators for harvesting biomechanical energy and as self-powered active tactile sensor system," *ACS Nano*, vol. 7, no. 10, 2013, doi: 10.1021/nn403838y.

[20] X. Gang *et al.*, "Textile Triboelectric Nanogenerators Simultaneously Harvesting Multiple 'High-Entropy' Kinetic Energies," *ACS Appl. Mater. Interfaces*, vol. 13, no. 17, pp. 20145–20152, 2021, doi: 10.1021/acsami.1c03250.

[21] M. Salauddin and J. Y. Park, "Design and experiment of human hand motion driven electromagnetic energy harvester using dual Halbach magnet array," *Smart Mater. Struct.*, vol. 26, no. 3, 2017, doi: 10.1088/1361-665X/aa573f.

[22] F. Qian, T. B. Xu, and L. Zuo, "Design, optimization, modeling and testing of a piezoelectric footwear energy harvester," *Energy Convers. Manag.*, vol. 171, 2018, doi: 10.1016/j.enconman.2018.06.069.

[23] F. Guido, A. Qualtieri, L. Algieri, E. D. Lemma, M. De Vittorio, and M. T. Todaro, "AlN-based flexible piezoelectric skin for energy harvesting from human motion," *Microelectron. Eng.*, vol. 159, 2016, doi: 10.1016/j.mee.2016.03.041.

[24] H. Fu *et al.*, "Footstep energy harvesting using heel strike-induced airflow for human activity sensing," *BSN 2016 - 13th Annu. Body Sens. Networks Conf.*, no. June, pp. 124–129, 2016, doi: 10.1109/BSN.2016.7516245.

[25] C. Rodrigues *et al.*, "Emerging triboelectric nanogenerators for ocean wave energy harvesting: state of the art and future perspectives," *Energy Environ. Sci.*, vol. 13, no. 9, pp. 2657–2683, 2020, doi: 10.1039/d0ee01258k.

[26] C. Dagdeviren, Z. Li, and Z. L. Wang, "Energy Harvesting from the Animal-Human Body for Self-Powered Electronics," *Annu. Rev. Biomed. Eng.*, vol. 19, pp. 85–108, 2017, doi: 10.1146/annurev-bioeng-071516-044517.

[27] C. Sukumaran, P. Viswanathan, P. Munirathinam, and A. Chandrasekhar, "A

flexible and wearable joint motion sensor using triboelectric nanogenerators for hand gesture monitoring," in *International Journal of Nanotechnology*, 2021, vol. 18, no. 5–8. doi: 10.1504/IJNT.2021.116183.

[28] K. Venugopal, P. Panchatcharam, A. Chandrasekhar, and V. Shanmugasundaram, "Comprehensive Review on Triboelectric Nanogenerator Based Wrist Pulse Measurement: Sensor Fabrication and Diagnosis of Arterial Pressure," *ACS Sensors*, vol. 6, no. 5, 2021, doi: 10.1021/acssensors.0c02324.

[29] W. Fan *et al.*, "Machine-knitted washable sensor array textile for precise epidermal physiological signal monitoring," *Sci. Adv.*, vol. 6, no. 11, pp. 1–11, 2020, doi: 10.1126/sciadv.aay2840.

[30] P. K. Yang *et al.*, "Paper-based origami triboelectric nanogenerators and self-powered pressure sensors," *ACS Nano*, vol. 9, no. 1, 2015, doi: 10.1021/nn506631t.

[31] A. A. Mathew, S. Vivekanandan, and A. Chandrasekhar, "Nanogenerator-based Sensors for Human Pulse Measurement," in *Green Engineering and Technology*, 2021. doi: 10.1201/9781003176275-18.

[32] F. Sheng *et al.*, "Self-Powered Smart Arm Training Band Sensor Based on Extremely Stretchable Hydrogel Conductors," *ACS Appl. Mater. Interfaces*, vol. 13, no. 37, pp. 44868–44877, 2021, doi: 10.1021/acsami.1c12378.

[33] S. S. Sophie Bergerbrant, "A History of Ancient Textile Production," *Cambridge University Press*, 2019. https://www.cambridgeblog.org/2019/10/a-history-of-ancient-textile-production/#:~:text=The first traces of textiles,survive in the archaeological record.

[34] S. Dong, F. Xu, Y. Sheng, Z. Guo, X. Pu, and Y. Liu, "Seamlessly knitted stretchable comfortable textile triboelectric nanogenerators for E-textile power sources," *Nano Energy*, vol. 78, p. 105327, Dec. 2020, doi: 10.1016/J.NANOEN.2020.105327.

[35] L. Chen *et al.*, "Stretchable negative Poisson's ratio yarn for triboelectric

nanogenerator for environmental energy harvesting and self-powered sensor," *Energy Environ. Sci.*, vol. 14, no. 2, pp. 955–964, 2021, doi: 10.1039/d0ee02777d.

[36] J. Xiong *et al.*, "Skin-touch-actuated textile-based triboelectric nanogenerator with black phosphorus for durable biomechanical energy harvesting," *Nat. Commun.*, vol. 9, no. 1, pp. 1–9, 2018, doi: 10.1038/s41467-018-06759-0.

[37] "Scalable fabrication of stretchable and washable textile triboelectric.pdf."

[38] M. Zhu *et al.*, "3D spacer fabric based multifunctional triboelectric nanogenerator with great feasibility for mechanized large-scale production," *Nano Energy*, vol. 27, pp. 439–446, Sep. 2016, doi: 10.1016/J.NANOEN.2016.07.016.

[39] D. Dassanayaka, D. Hedigalla, and U. Gunasekera, "Biodegradable Composite for Temporary Partitioning Materials," *MERCon 2020 - 6th Int. Multidiscip. Moratuwa Eng. Res. Conf. Proc.*, pp. 453–458, 2020, doi: 10.1109/MERCon50084.2020.9185232.

[40] Y. Zou, L. Bo, and Z. Li, "Recent progress in human body energy harvesting for smart bioelectronic system," *Fundam. Res.*, vol. 1, no. 3, pp. 364–382, 2021, doi: 10.1016/j.fmre.2021.05.002.

[41] "No Title," *britannica*. [Online]. Available: https://www.britannica.com/science/adenosine-triphosphate

[42] C. Rodrigues, A. Gomes, A. Ghosh, A. Pereira, and J. Ventura, "Power-generating footwear based on a triboelectric-electromagnetic-piezoelectric hybrid nanogenerator," *Nano Energy*, vol. 62, no. January, pp. 660–666, 2019, doi: 10.1016/j.nanoen.2019.05.063.

[43] R. E. Newnham, *COMPOSITE ELECTROCERAMICS.*, vol. 16. 1986.

[44] S. Chen *et al.*, "A Single Integrated 3D-Printing Process Customizes Elastic and Sustainable Triboelectric Nanogenerators for Wearable Electronics," *Adv. Funct. Mater.*, vol. 28, no. 46, 2018, doi: 10.1002/adfm.201805108.

[45] Z. L. Wang, “Triboelectric nanogenerators as new energy technology and self-powered sensors - Principles, problems and perspectives,” *Faraday Discussions*, vol. 176, no. 0. Royal Society of Chemistry, pp. 447–458, 2015. doi: 10.1039/c4fd00159a.

[46] R. D. I. G. Dharmasena, K. D. G. I. Jayawardena, C. A. Mills, R. A. Dorey, and S. R. P. Silva, “A unified theoretical model for Triboelectric Nanogenerators,” *Nano Energy*, vol. 48, pp. 391–400, Jun. 2018, doi: 10.1016/j.nanoen.2018.03.073.

[47] R. D. I. G. Dharmasena, J. H. B. Deane, and S. R. P. Silva, “Nature of Power Generation and Output Optimization Criteria for Triboelectric Nanogenerators,” *Adv. Energy Mater.*, p. 1802190, Sep. 2018, doi: 10.1002/aenm.201802190.

[48] R. D. I. G. Dharmasena *et al.*, “Triboelectric nanogenerators: providing a fundamental framework,” *Energy Environ. Sci.*, vol. 10, no. 8, pp. 1801–1811, 2017, doi: 10.1039/C7EE01139C.

[49] Z. L. Wang, “On Maxwell’s displacement current for energy and sensors: the origin of nanogenerators,” *Materials Today*, vol. 20, no. 2. pp. 74–82, 2017. doi: 10.1016/j.mattod.2016.12.001.

[50] S. Niu *et al.*, “Theoretical study of contact-mode triboelectric nanogenerators as an effective power source,” *Energy Environ. Sci.*, vol. 6, no. 12, pp. 3576–3583, 2013, doi: 10.1039/c3ee42571a.

[51] S. Niu *et al.*, “Theory of Sliding-Mode Triboelectric Nanogenerators,” *Adv. Mater.*, vol. 25, no. 43, pp. 6184–6193, Nov. 2013, doi: 10.1002/adma.201302808.

[52] S. Niu *et al.*, “Theory of freestanding triboelectric-layer-based nanogenerators,” *Nano Energy*, vol. 12, pp. 760–774, 2015, doi: 10.1016/j.nanoen.2015.01.013.

[53] S. Niu *et al.*, “Theoretical Investigation and Structural Optimization of Single-Electrode Triboelectric Nanogenerators,” *Adv. Funct. Mater.*, vol. 24, no. 22,

pp. 3332–3340, Jun. 2014, doi: 10.1002/adfm.201303799.

[54] R. Dharmasena, “Inherent asymmetry of the current output in a triboelectric nanogenerator,” *Nano Energy*, p. 105045, 2020.

[55] R. D. I. G. Dharmasena, “Triboelectric self-powered energy systems. [Doctoral Dissertation],” University of Surrey, 2019.

[56] J. Shao, M. Willatzen, Y. Shi, and Z. L. Wang, “3D mathematical model of contact-separation and single-electrode mode triboelectric nanogenerators,” *Nano Energy*, vol. 60, pp. 630–640, 2019.

[57] J. Shao, M. Willatzen, and Z. L. Wang, “Theoretical modeling of triboelectric nanogenerators (TENGs),” *J. Appl. Phys.*, vol. 128, no. 11, p. 111101, 2020.

[58] J. Chen *et al.*, “Enhancing Performance of Triboelectric Nanogenerator by Filling High Dielectric Nanoparticles into Sponge PDMS Film,” *ACS Appl. Mater. Interfaces*, vol. 8, no. 1, pp. 736–744, Jan. 2016, doi: 10.1021/acsami.5b09907.

[59] N. Cui *et al.*, “Dynamic Behavior of the Triboelectric Charges and Structural Optimization of the Friction Layer for a Triboelectric Nanogenerator,” *ACS Nano*, vol. 10, no. 6, pp. 6131–6138, Jun. 2016, doi: 10.1021/acsnano.6b02076.

[60] M.-L. Seol, S.-H. Lee, J.-W. Han, D. Kim, G.-H. Cho, and Y.-K. Choi, “Impact of contact pressure on output voltage of triboelectric nanogenerator based on deformation of interfacial structures,” *Nano Energy*, vol. 17, pp. 63–71, Oct. 2015, doi: 10.1016/J.NANOEN.2015.08.005.

[61] V. Nguyen and R. Yang, “Effect of humidity and pressure on the triboelectric nanogenerator,” *Nano Energy*, vol. 2, no. 5, pp. 604–608, Sep. 2013, doi: 10.1016/J.NANOEN.2013.07.012.

[62] C. Xu *et al.*, “On the Electron-Transfer Mechanism in the Contact-Electrification Effect,” *Adv. Mater.*, vol. 30, no. 15, p. 1706790, Mar. 2018, doi: 10.1002/adma.201706790.

[63] G. Zhu *et al.*, “Toward Large-Scale Energy Harvesting by a Nanoparticle-Enhanced Triboelectric Nanogenerator,” *Nano Lett.*, vol. 13, no. 2, pp. 847–853, Feb. 2013, doi: 10.1021/nl4001053.

[64] B. Chen, Y. Yang, and Z. L. Wang, “Scavenging Wind Energy by Triboelectric Nanogenerators,” *Advanced Energy Materials*, vol. 8, no. 10. 2018. doi: 10.1002/aenm.201702649.

[65] S. Wang, S. Niu, J. Yang, L. Lin, and Z. L. Wang, “Quantitative measurements of vibration amplitude using a contact-mode freestanding triboelectric nanogenerator,” *ACS Nano*, vol. 8, no. 12, 2014, doi: 10.1021/nn5054365.

[66] X. Peng *et al.*, “All-Nanofiber Self-Powered Skin-Interfaced Real-Time Respiratory Monitoring System for Obstructive Sleep Apnea-Hypopnea Syndrome Diagnosing,” *Adv. Funct. Mater.*, vol. 31, no. 34, 2021, doi: 10.1002/adfm.202103559.

[67] Y. Li *et al.*, “Mechanically interlocked stretchable nanofibers for multifunctional wearable triboelectric nanogenerator,” *Nano Energy*, vol. 78, no. August, 2020, doi: 10.1016/j.nanoen.2020.105358.

[68] L. Ma *et al.*, “Continuous and Scalable Manufacture of Hybridized Nano-Micro Triboelectric Yarns for Energy Harvesting and Signal Sensing,” *ACS Nano*, vol. 14, no. 4, pp. 4716–4726, 2020, doi: 10.1021/acsnano.0c00524.

[69] M. Joshi and B. S. Butola, “Application technologies for coating, lamination and finishing of technical textiles,” *Adv. Dye. Finish. Tech. Text.*, pp. 355–411, Jan. 2013, doi: 10.1533/9780857097613.2.355.

[70] C. Ning *et al.*, “Flexible and Stretchable Fiber-Shaped Triboelectric Nanogenerators for Biomechanical Monitoring and Human-Interactive Sensing,” *Adv. Funct. Mater.*, vol. 31, no. 4, pp. 1–9, 2021, doi: 10.1002/adfm.202006679.

[71] C. Emonts *et al.*, “Innovation in 3D Braiding Technology and Its Applications,” *Textiles*, vol. 1, no. 2, pp. 185–205, 2021, doi:

10.3390/textiles1020009.

[72] K. Dong *et al.*, “Shape adaptable and highly resilient 3D braided triboelectric nanogenerators as e-textiles for power and sensing,” *Nat. Commun.*, vol. 11, no. 1, pp. 1–11, 2020, doi: 10.1038/s41467-020-16642-6.

[73] H. Gebeyehu Menge, S. Hyun Jo, and Y. Tae Park, “Layer-by-Layer Self-Assembled Thin Films for Triboelectric Energy Harvesting under Harsh Conditions,” *ACS Appl. Electron. Mater.*, vol. 3, no. 12, pp. 5475–5482, Nov. 2021, doi: 10.1021/acsaelm.1c00907.

[74] J. Chen, H. Guo, X. Pu, X. Wang, Y. Xi, and C. Hu, “Traditional weaving craft for one-piece self-charging power textile for wearable electronics,” *Nano Energy*, vol. 50, pp. 536–543, Aug. 2018, doi: 10.1016/J.NANOEN.2018.06.009.

[75] Y. H. Ko, G. Nagaraju, and J. S. Yu, “Multi-stacked PDMS-based triboelectric generators with conductive textile for efficient energy harvesting,” *RSC Adv.*, vol. 5, no. 9, pp. 6437–6442, 2015, doi: 10.1039/c4ra15310c.

[76] X. Pu *et al.*, “Wearable Self-Charging Power Textile Based on Flexible Yarn Supercapacitors and Fabric Nanogenerators,” *Adv. Mater.*, vol. 28, no. 1, pp. 98–105, 2016, doi: 10.1002/adma.201504403.

[77] B. N. Chandrashekar *et al.*, “Roll-to-Roll Green Transfer of CVD Graphene onto Plastic for a Transparent and Flexible Triboelectric Nanogenerator,” *Adv. Mater.*, vol. 27, no. 35, pp. 5210–5216, 2015, doi: 10.1002/adma.201502560.

[78] R. Cheng *et al.*, “Flame-retardant textile-based triboelectric nanogenerators for fire protection applications,” *ACS Nano*, vol. 14, no. 11, pp. 15853–15863, 2020, doi: 10.1021/acsnano.0c07148.

[79] J. Yi *et al.*, “Fully Fabric-Based Triboelectric Nanogenerators as Self-Powered Human–Machine Interactive Keyboards,” *Nano-Micro Lett.*, vol. 13, no. 1, p. 103, Dec. 2021, doi: 10.1007/s40820-021-00621-7.

[80] R. D. I. Dharmasena, “Scalable Textile Manufacturing Methods for

Fabricating Triboelectric Nanogenerators with Balanced Electrical and Wearable Properties," 2022, doi: 10.1021/acsaelm.1c01095.

[81] D. Doganay *et al.*, "Fabric based wearable triboelectric nanogenerators for human machine interface," *Nano Energy*, vol. 89, Nov. 2021.

[82] B. Charroux, F. Daian, and J. Royet, "Drosophila Aversive Behavior toward Erwinia carotovora carotovora Is Mediated by Bitter Neurons and Leukokinin," *iScience*, vol. 23, no. 6, p. 101152, 2020, doi: 10.1016/j.isci.

[83] E. He *et al.*, "3D angle-interlock woven structural wearable triboelectric nanogenerator fabricated with silicone rubber coated graphene oxide/cotton composite yarn," *Compos. Part B Eng.*, vol. 200, no. April, p. 108244, 2020, doi: 10.1016/j.compositesb.2020.108244.

[84] V. U. Somkuwar, A. Pragya, and B. Kumar, "Structurally engineered textile-based triboelectric nanogenerator for energy harvesting application," *J. Mater. Sci.*, vol. 55, no. 12, pp. 5177–5189, 2020, doi: 10.1007/s10853-020-04359-2.

[85] T. Huang *et al.*, "Fabric texture design for boosting the performance of a knitted washable textile triboelectric nanogenerator as wearable power," *Nano Energy*, vol. 58, pp. 375–383, 2019, doi: 10.1016/j.nanoen.2019.01.038.

[86] C. Chen *et al.*, "3D double-faced interlock fabric triboelectric nanogenerator for bio-motion energy harvesting and as self-powered stretching and 3D tactile sensors," *Mater. Today*, vol. 32, no. xx, pp. 84–93, 2020, doi: 10.1016/j.mattod.2019.10.025.

[87] F. Xu *et al.*, "Scalable fabrication of stretchable and washable textile triboelectric nanogenerators as constant power sources for wearable electronics," *Nano Energy*, vol. 88, no. May, p. 106247, 2021, doi: 10.1016/j.nanoen.2021.106247.

[88] D. J. Spencer, *Knitting Technology*. 1983.

[89] L. Ma *et al.*, "A Machine-Fabricated 3D Honeycomb-Structured Flame-Retardant Triboelectric Fabric for Fire Escape and Rescue," *Adv. Mater.*, vol.

32, no. 38, pp. 1–10, 2020, doi: 10.1002/adma.202003897.

[90] S. Materials, “d M pt,” 2020.

[91] “What is IoT?” https://www.oracle.com/internet-of-things/what-is-iot/

[92] N. Y. Philip, J. J. P. C. Rodrigues, H. Wang, S. J. Fong, and J. Chen, “Internet of Things for In-Home Health Monitoring Systems: Current Advances, Challenges and Future Directions,” *IEEE J. Sel. Areas Commun.*, vol. 39, no. 2, pp. 300–310, 2021, doi: 10.1109/JSAC.2020.3042421.

[93] W. H. Organization, *mHealth: new horizons for health through mobile technologies: second global survey on eHealth*, 3rd ed. World Health Organization, 2011. [Online]. Available: https://apps.who.int/iris/handle/10665/44607

[94] R. Alexandre and O. Postolache, “Wearable and IoT Technologies Application for Physical Rehabilitation,” *2018 Int. Symp. Sens. Instrum. IoT Era, ISSI 2018*, pp. 1–6, 2018, doi: 10.1109/ISSI.2018.8538058.

[95] H. Zou *et al.*, “Quantifying the triboelectric series,” *Nat. Commun.*, vol. 10, no. 1, p. 1427, Dec. 2019, doi: 10.1038/s41467-019-09461-x.

[96] D. Liu, L. Zhou, Z. L. Wang, and J. Wang, “Triboelectric nanogenerator: from alternating current to direct current,” *iScience*, vol. 24, no. 1, p. 102018, 2021, doi: 10.1016/j.isci.2020.102018.